

Multi-Scale Impacts of the Midlatitude Ocean on the Atmosphere

- An Overview of Processes Involved –

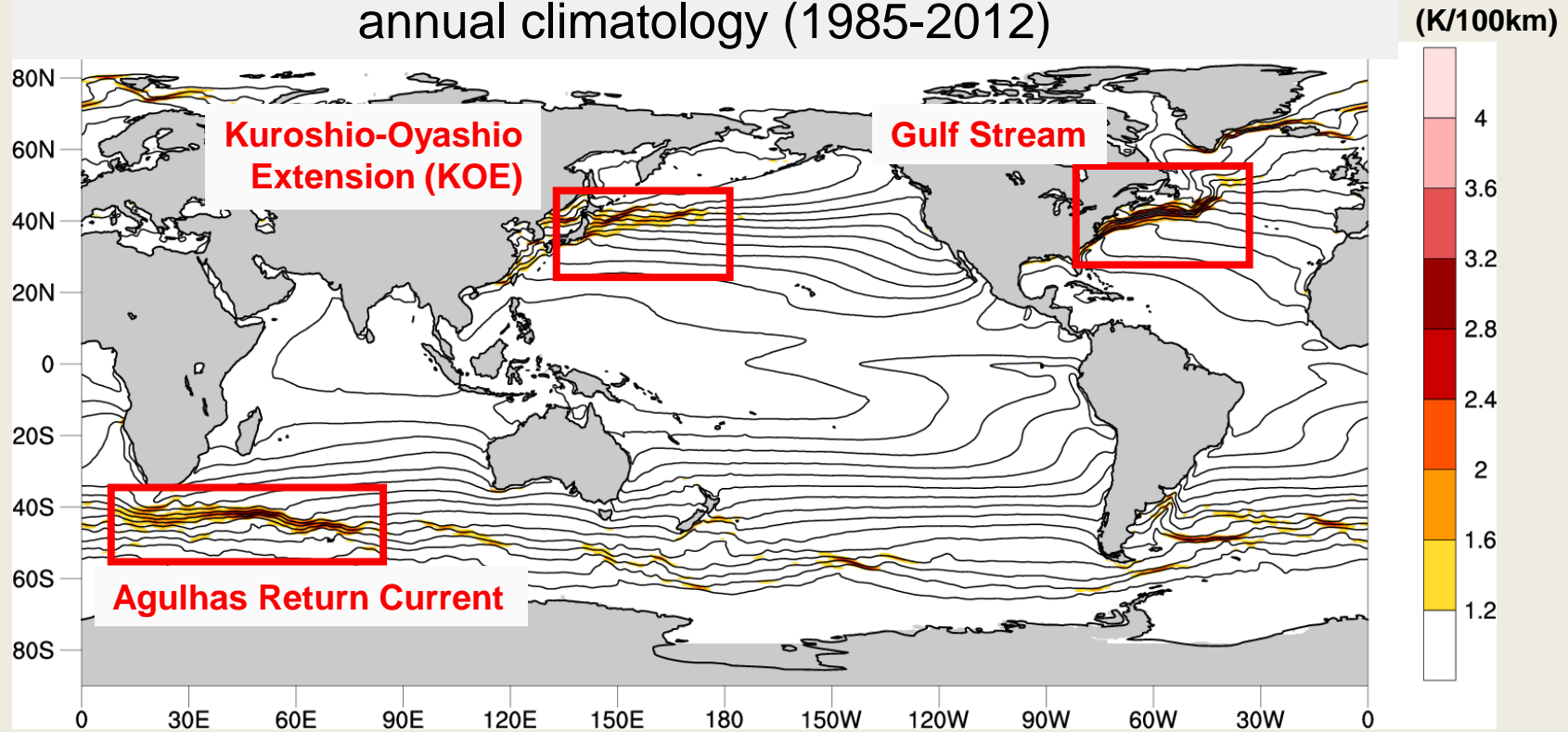
*Hisashi Nakamura

RCAST, University of Tokyo, also JAMSTEC

R. Masunaga, F. Ogawa, B. Taguchi, K. Nishii, M. Nonaka, T. Sampe, A. Manda, H. Kamahori, K. Onogi, A. Miyamoto, M. Koike, T. Miyasaka, S.-P. Xie, P. Chang, B. Qiu, R.J. Small, Y.-O. Kwon and L. Wu

Western Boundary Currents and midlatitude oceanic frontal zones

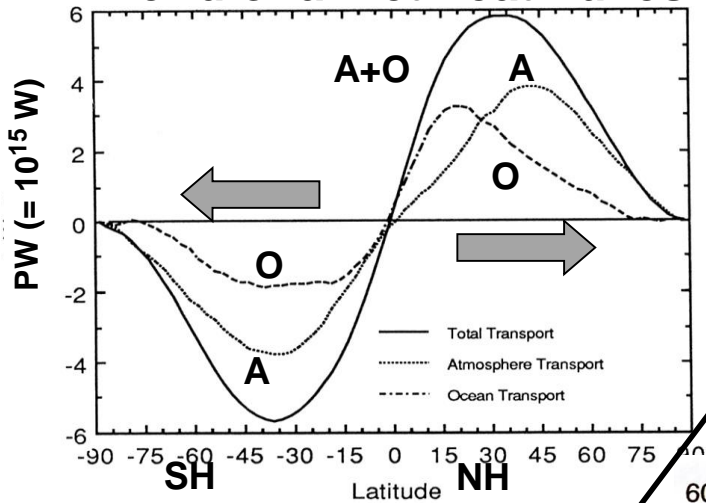
Satellite-measured SST(contour; MGDSSST), $|dSST/dy|$ (color)
annual climatology (1985-2012)



- All major midlatitude oceanic frontal zones (OFZs) with steep SST gradients are associated with warm western boundary currents (WBCs).
- As "climatic hotspots", these OFZs can influence the overlying atmosphere as identified by recent studies.

Ocean heat transport and oceanic frontal zones

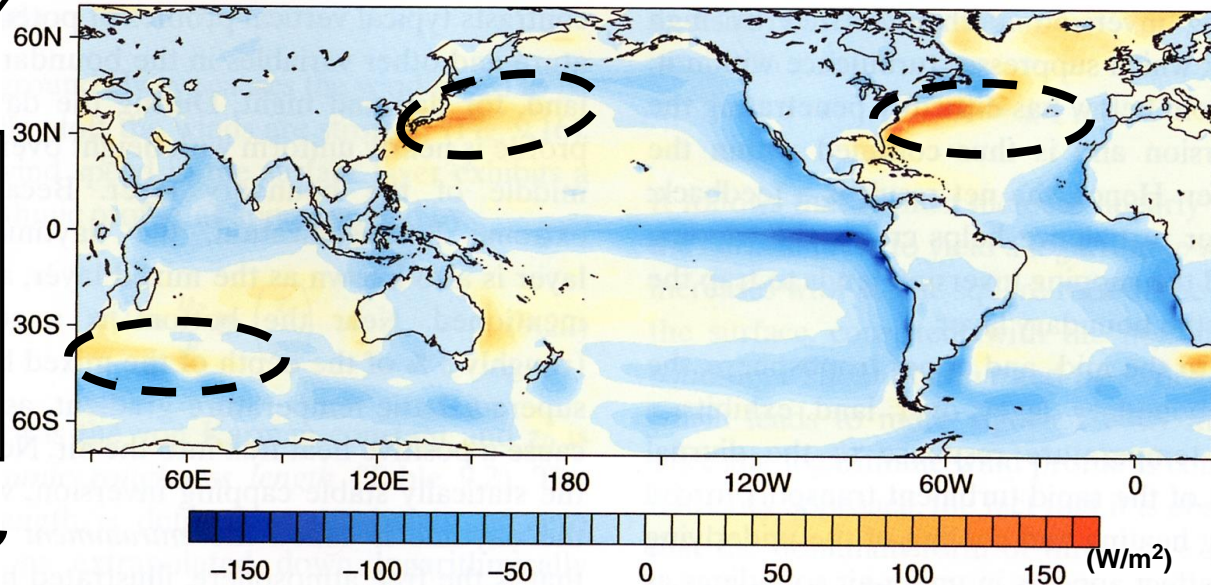
Meridional net heat fluxes



Warm WBCs* transport heat from the tropics into midlatitudes and then release it into the atmosphere **intensively from the warm WBCs** on the warmer sides of oceanic frontal zones.

“hotspots in the climate system”

Annual-mean net upward surface heat flux



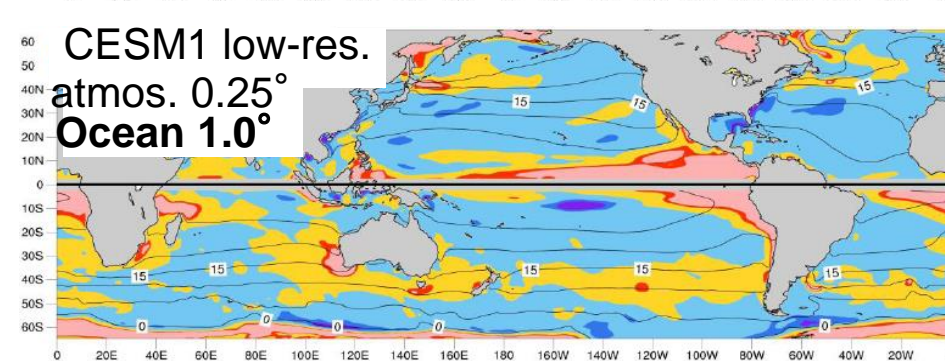
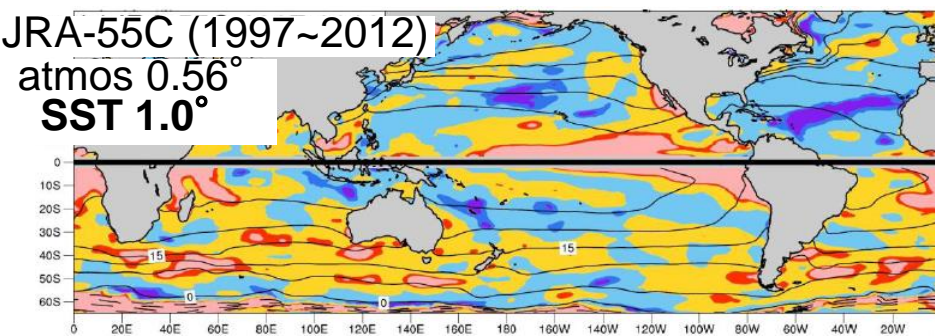
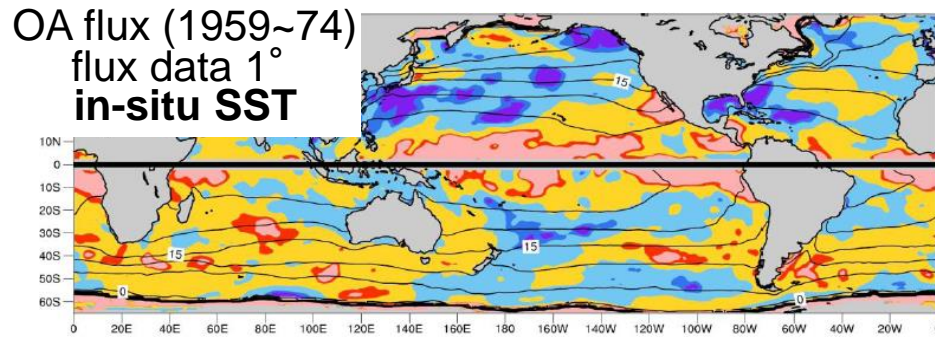
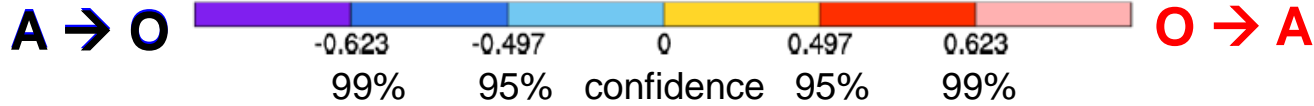
Then atmospheric eddies along stormtracks take over in heat transport into higher latitudes.



Major oceanic frontal zones where warm and cool currents are confluent.

*WBC: Western boundary current

Interannual correlation between SST and SHF+LHF for winter



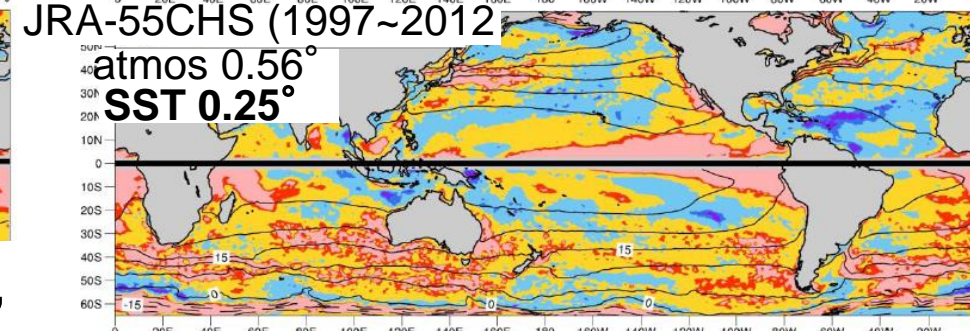
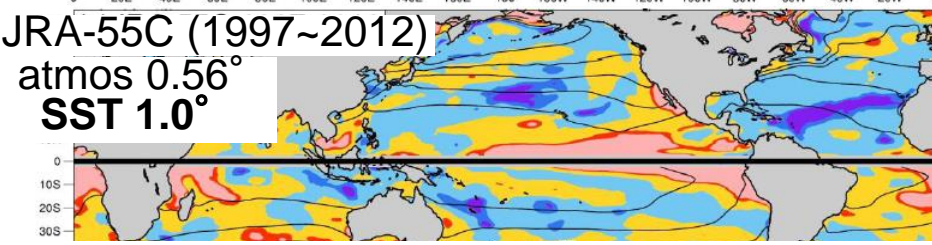
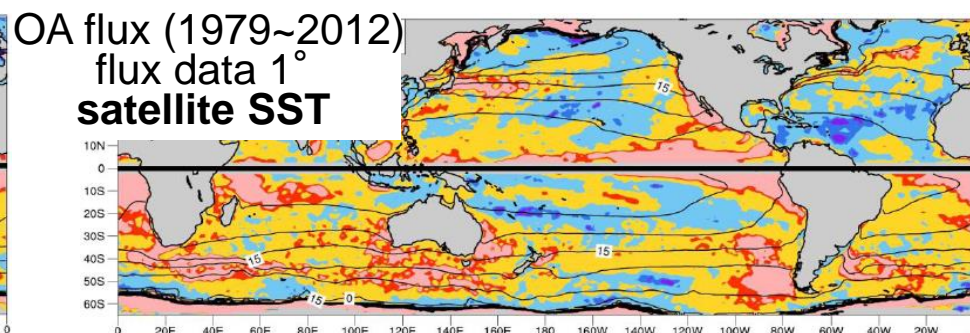
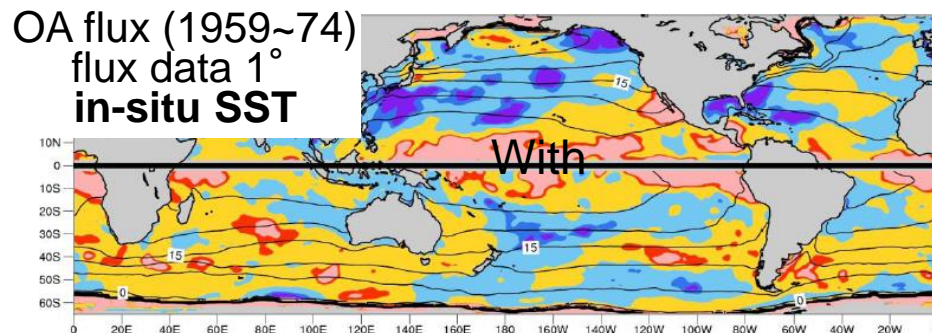
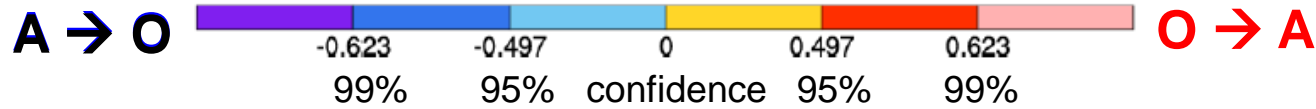
Local correlation between SST and turbulent heat fluxes (SHF, LHF) from the ocean indicates the primary direction of the forcing.

For **low-resolution SST** observed or simulated, the **correlation tends to be positive in the tropics**, indicative of **oceanic forcing** on the atmosphere.

By contrast, **negative correlation prevails in the extratropics**, indicative of the **atmospheric forcing** on the ocean.

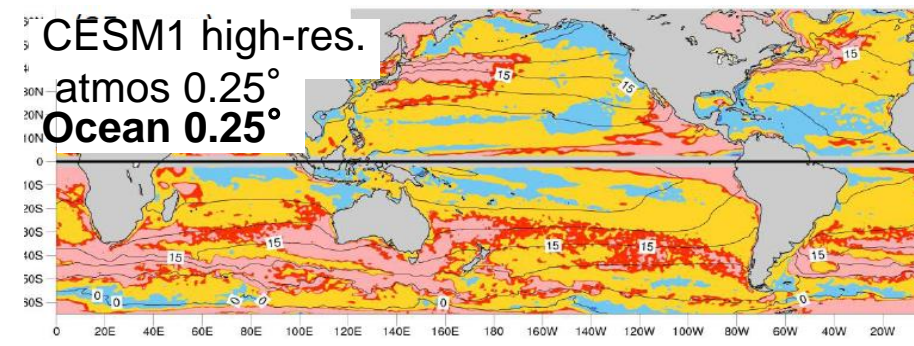
→ Conventional notion that the extratropical ocean is passive to the atmospheric variability.

Interannual correlation between SST and SHF+LHF for winter



For **high-resolution SST**, by contrast, its correlation with heat fluxes tends to be **positive** in both **the tropics and extratropics** (Bishop et al. 2017; Small et al. 2019).

→ **Active role of the midlatitude ocean in the climate system** (Tanimoto et al. 2003, Xie 2004).



Masunaga (2018)

Review papers: **Xie (2004 BAMS), Small et al. (2008 DAO), Chelton & Xie (2010 Oceanogr.), Kelly et al. (2010 JC), Kwon et al. (2010 JC)**

AMS special collection on
“Climate Implications of Frontal Scale Air-Sea Interaction”
(Short title: Frontal air-sea)
JC, MWR, JTECH, JPO etc.

Organizers:

Small, Alexander, Newman, Smirnov, Frankignoul, Kwon, Nakamura

Special section in ***J. Oceanography*** on
“Hot Spots” in the Climate System : New Developments in the
Extratropical Ocean-Atmosphere Interaction Research”,
published in October 2015.

*Spinoff books become available from Springer in 2016 spring.

Editors:

Nakamura, Isobe, Minobe, Mitsudera, Nonaka, Suga

Multi-Scale Impacts of the Midlatitude Ocean on the Atmosphere

- An Overview of Processes Involved –

1. *Introduction*
2. Fundamentals
3. Understanding local atmospheric response to SST fronts
4. Atmospheric response to decadal SST-front variability
5. SST front influence on low-cloud properties
6. *SST front influence on the Southern Annular Mode*
7. Comments on high-resolution modeling
8. Concluding remarks

Local influence of SST front on atmospheric boundary layer

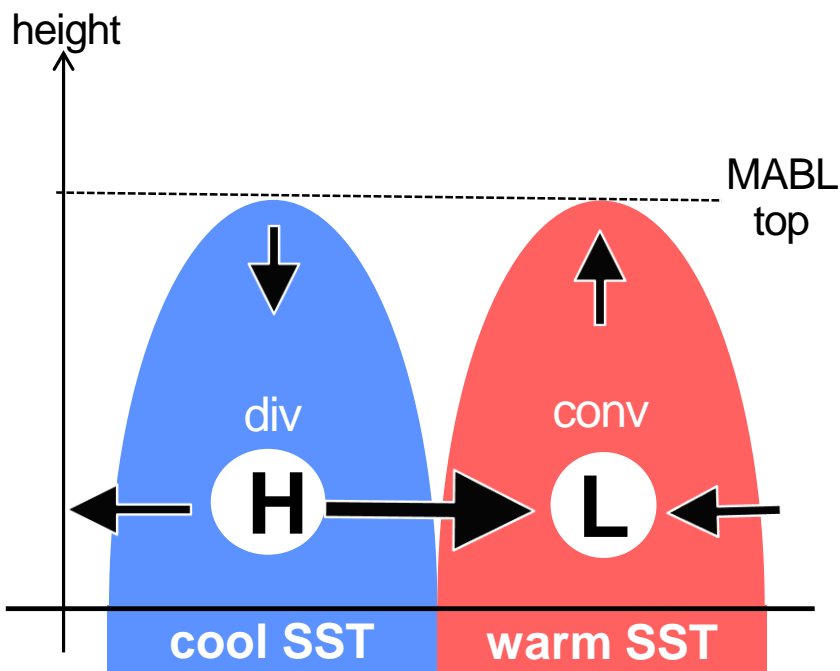
Pressure adjustment

(Lindzen & Nigam 1987)

Warm SST heats MABL

→ **lowered SLP** induces surface wind convergence and ascent aloft

effective for airflow **parallel** to front



SST

front

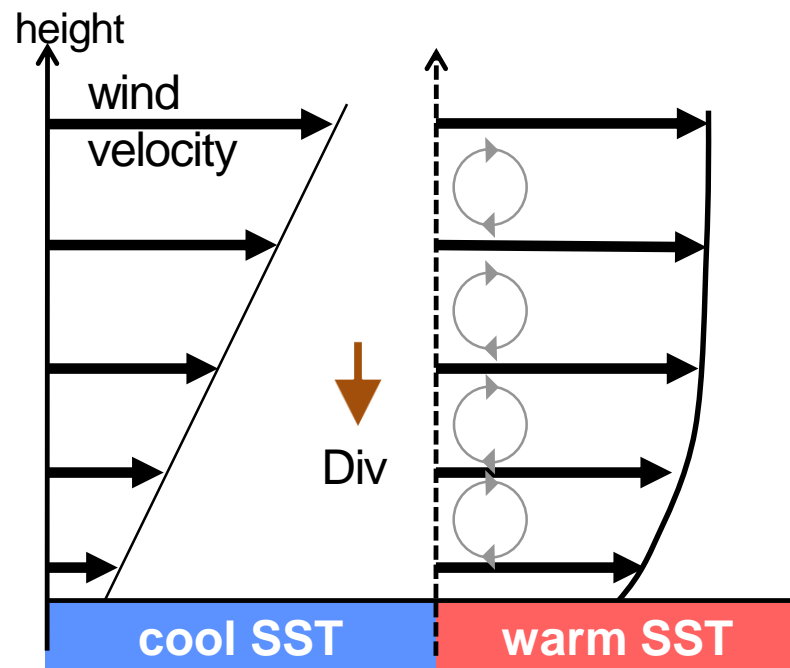
Vertical mixing

(Wallace et al. 1989; Hayes et al. 1989)

Warm SST destabilizes MABL

→ **enhanced downward transport of wind momentum**

→ surface airflow is accelerated on **crossing** from cool to warm SST



SST

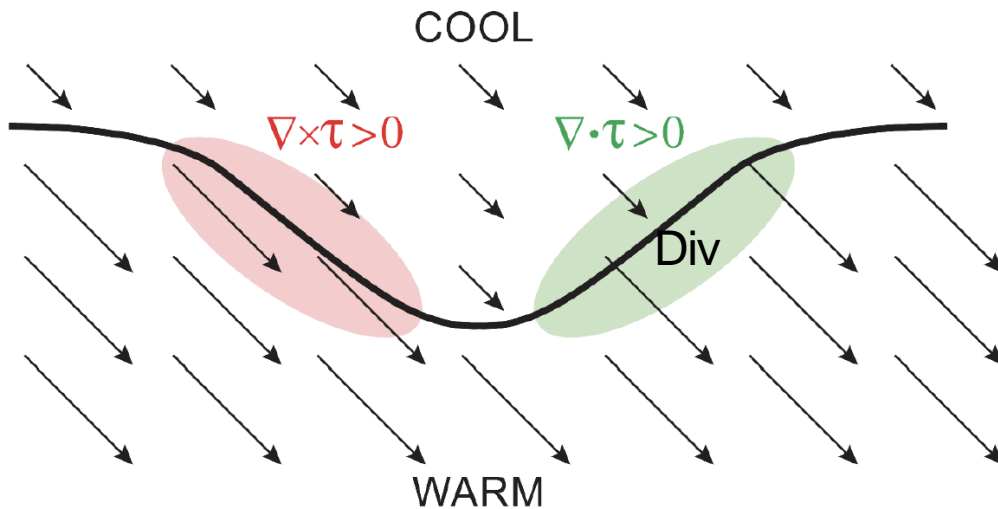
front

c.f. Takatama et al. (2012),
Masunaga (2018)

Local influence of SST front on atmospheric boundary layer

Spatially different response of surface wind to meandering SST front

(by ocean eddies)



Chelton et al. (2004)

Comprehensive analysis is given by Kilpatrick et al. (2014, 2016) and Schneider, Qiu (2015).

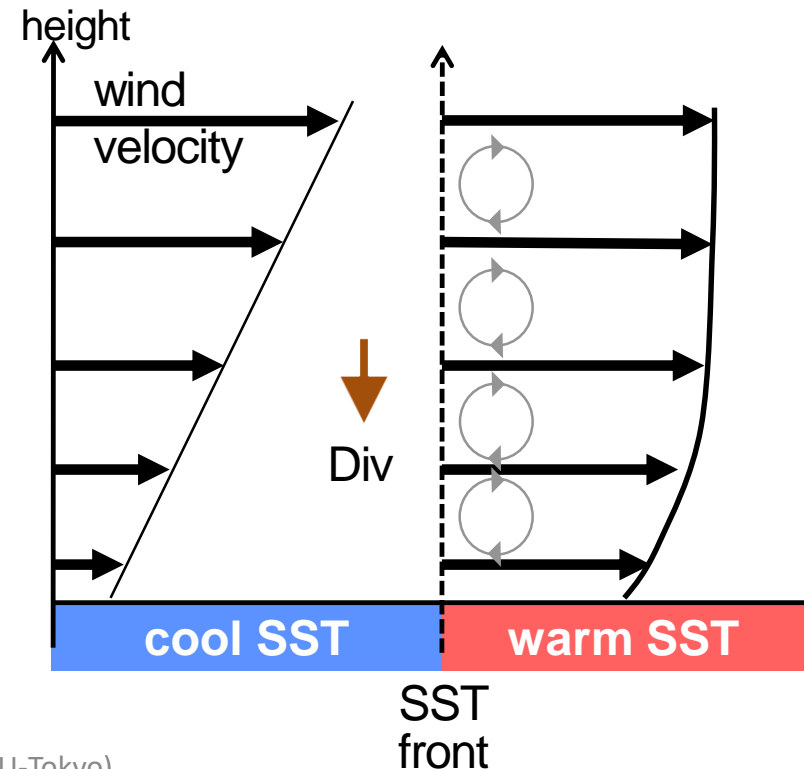
Vertical mixing

(Wallace et al. 1989; Hayes et al. 1989)

Warm SST destabilizes MABL

→ enhanced downward transport of wind momentum

→ surface airflow is accelerated on **crossing** from cool to warm SST



Local influence of SST front on atmospheric boundary layer

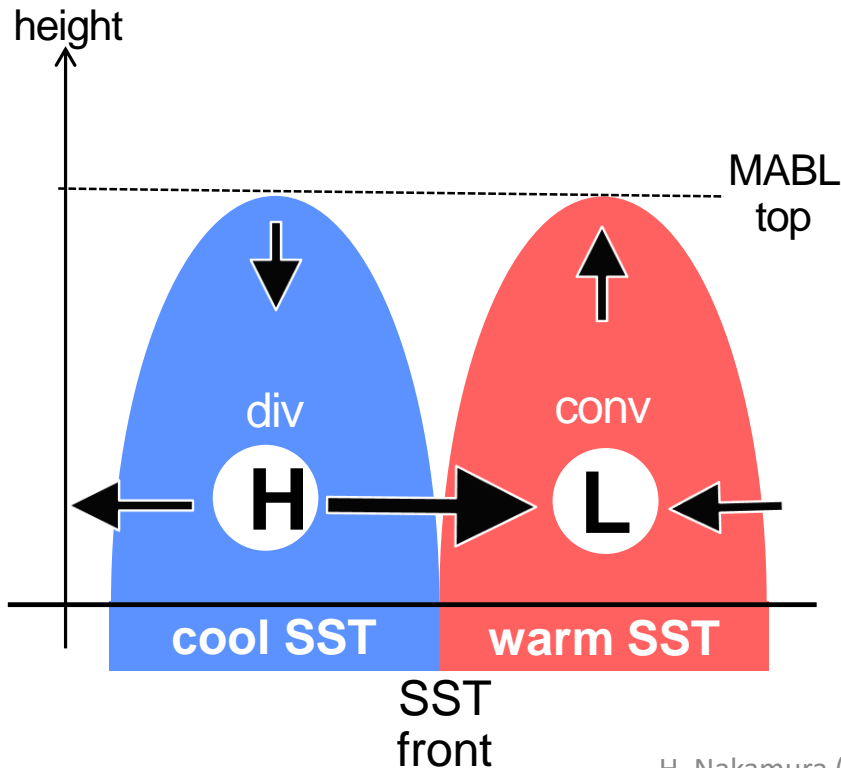
Pressure adjustment

(Lindzen & Nigam 1987)

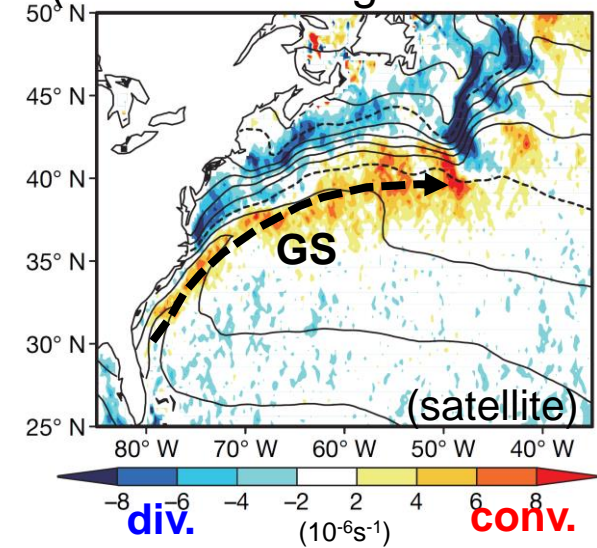
Warm SST heats MABL

→ lowered SLP induces surface wind convergence/ascent aloft

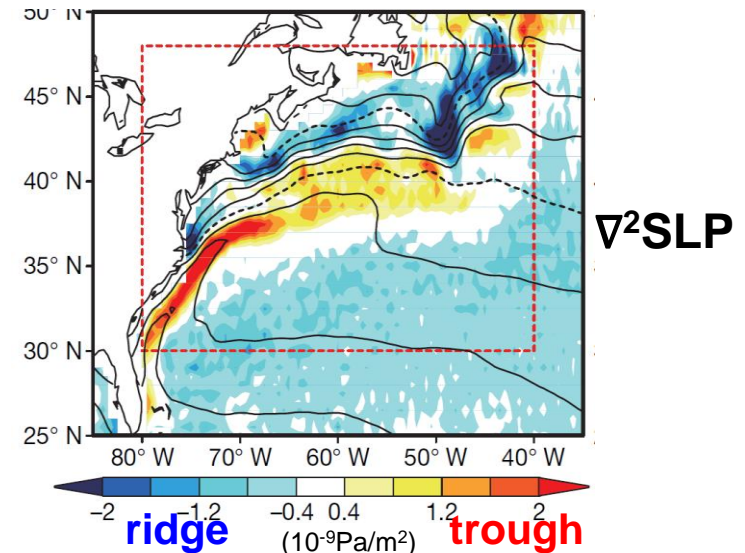
effective for airflow **parallel** to front



surface wind conv. along GS (with climatological rainband)

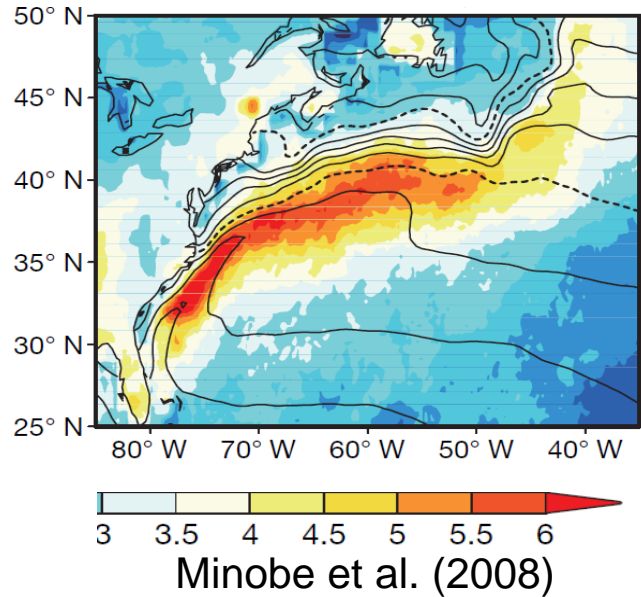


Minobe et al. (2008), O'Neil (2017)

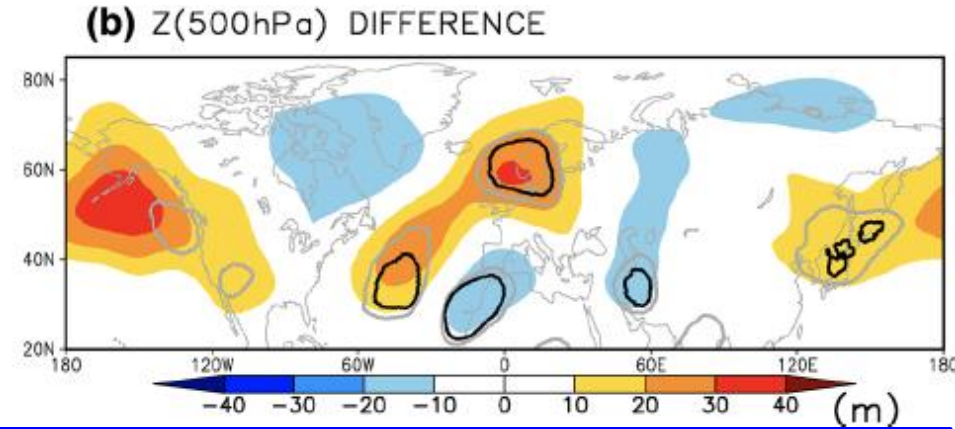


Local influence of SST front on atmospheric boundary layer

DJF precipitation climatology

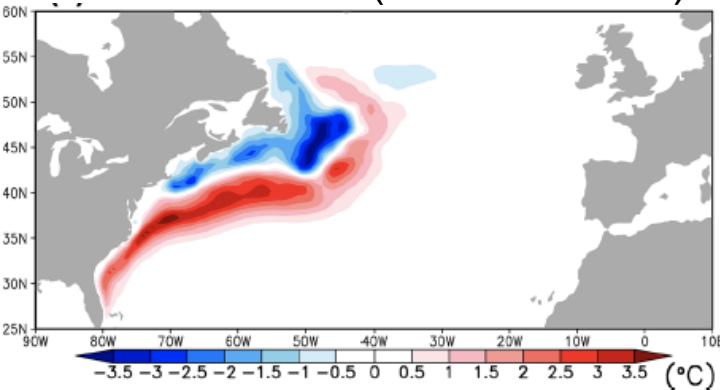


AGCM winter-mean response (CNTL–SMTH)



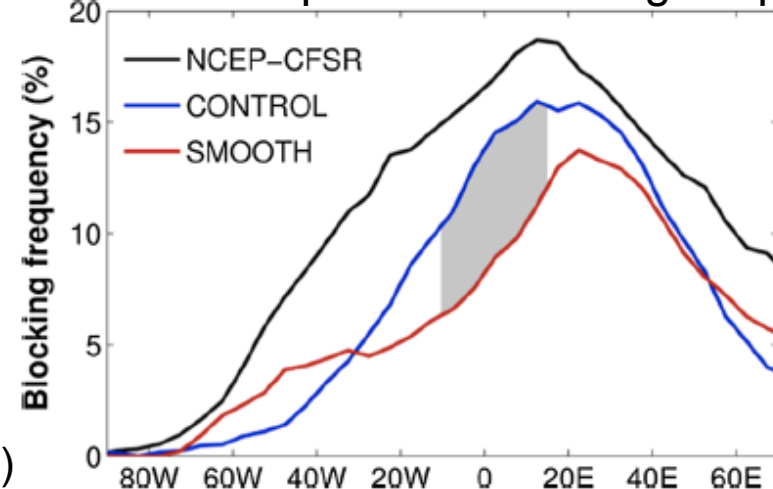
Enhanced precipitation along GS amplifies planetary-wave ridge over Europe, leading to increased blocking activity over Europe.

SST difference (CNTL–SMTH)



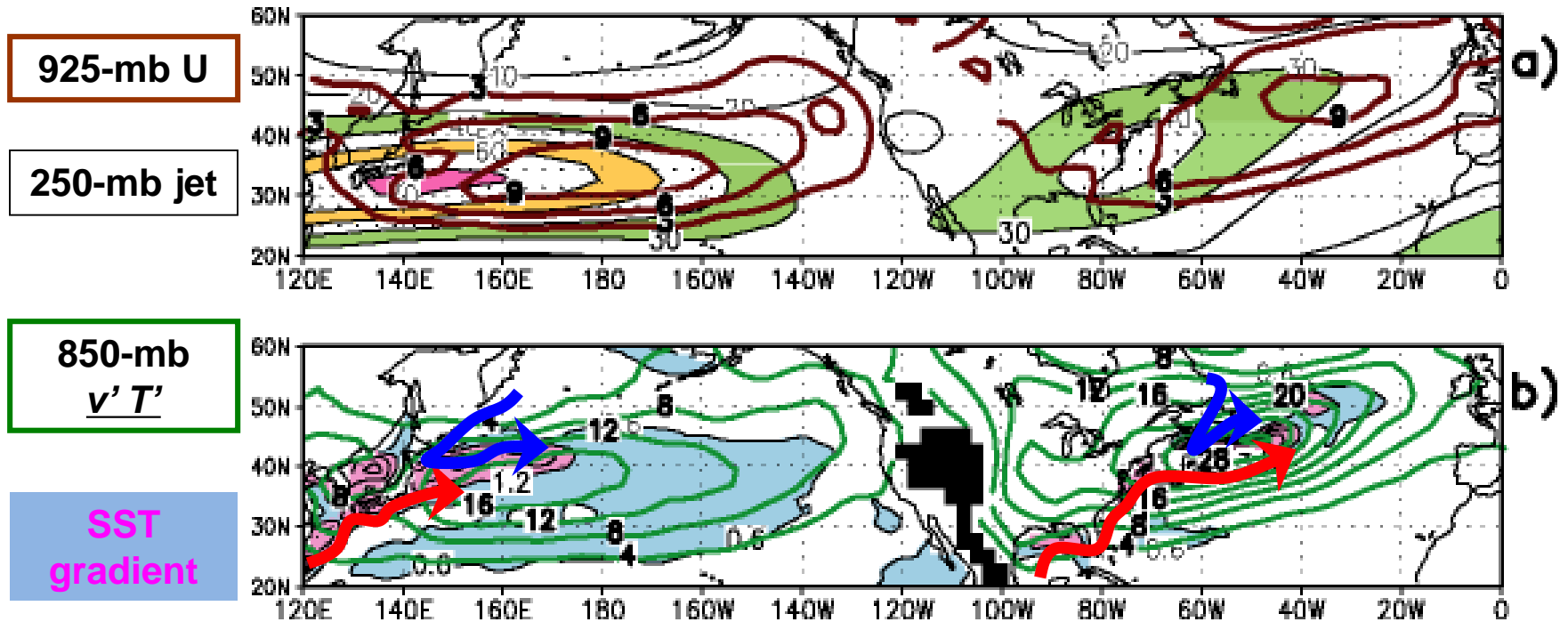
O'Reilly et al. (2017)

AGCM response in blocking freq.

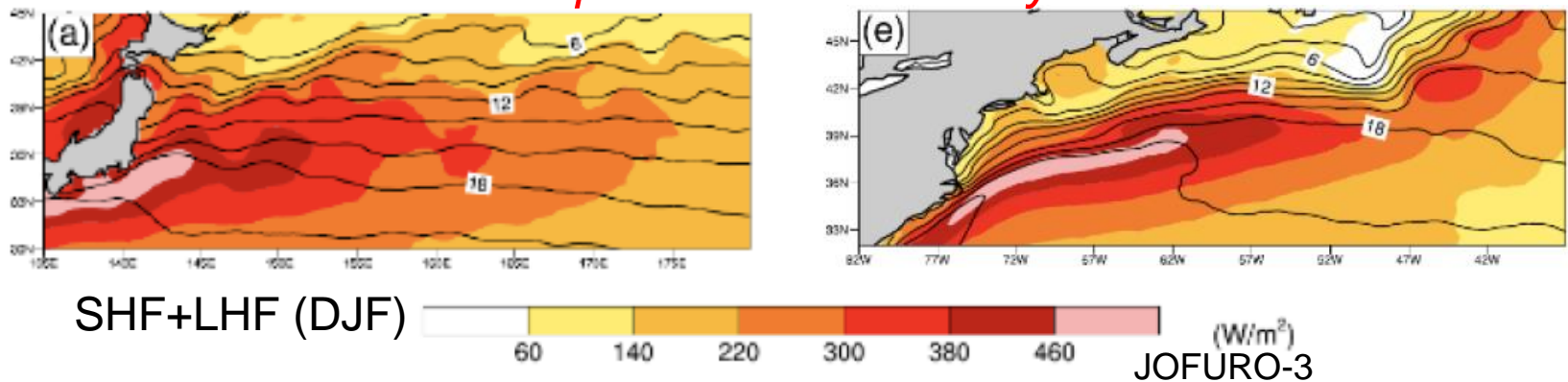


Stormtracks, surface westerlies and oceanic frontal zones in the wintertime Northern Hemisphere

Nakamura et al. (2004, AGU Geophys. Monogr.)

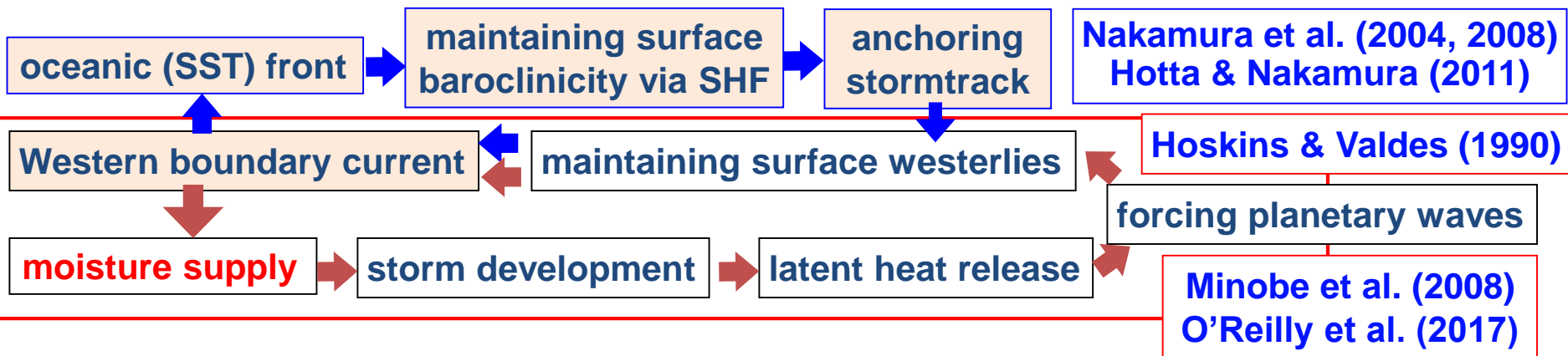
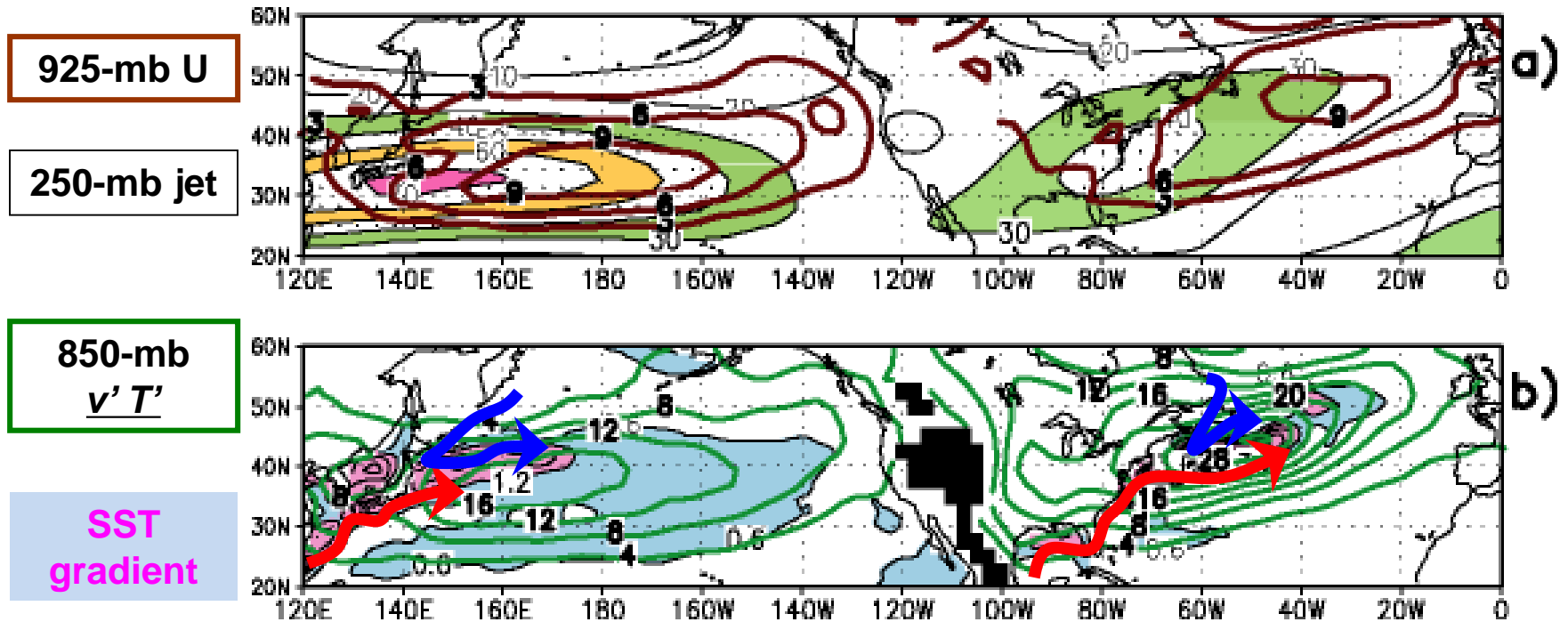


“hotspots in the climate system”



Stormtracks, surface westerlies and oceanic frontal zones in the wintertime Northern Hemisphere

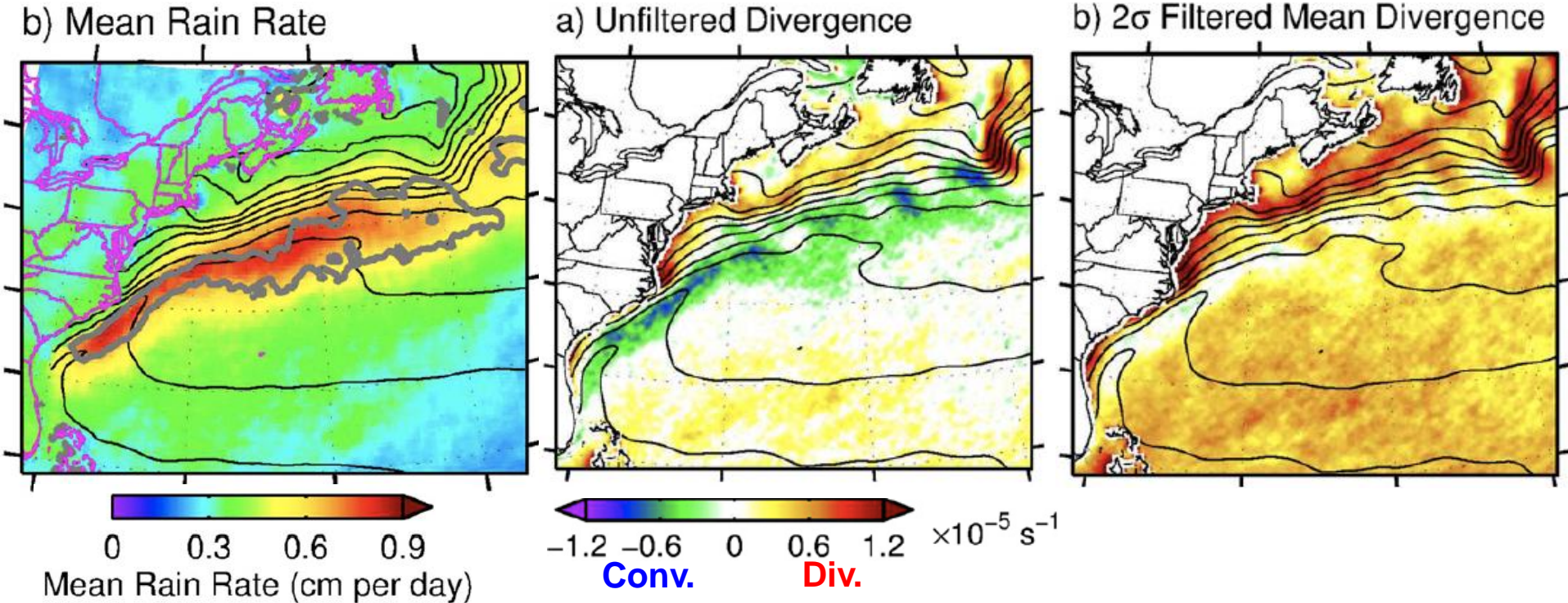
Nakamura et al. (2004, AGU Geophys. Monogr.)



Role of transient eddies in shaping mean surface conv./div.

annual-mean climatology (satellite)

Removal of very strong conv./div. due to transients

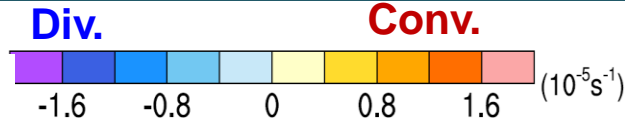
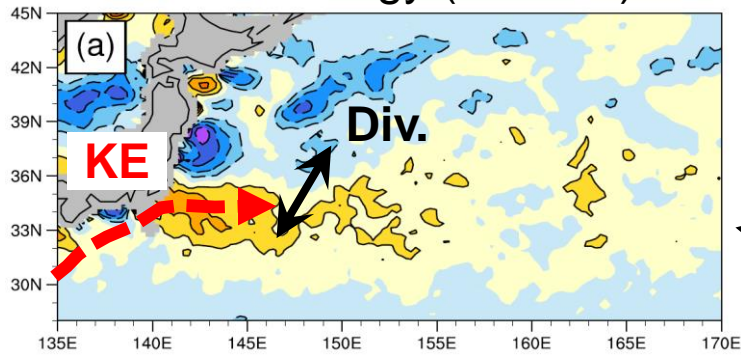


- Removal of effects of transient eddies lead to diminished conv. zone along GS
→ Role of strong cyclones is essential (O'Neil et al. 2017)
c.f. Parfitt & Czaja (2016); Parfitt et al. (2016)
- However, divergence on cool water is enhanced, and contrast across the GS front remains strong (Plougonven et al. 2018; Masunaga et al. 2019)

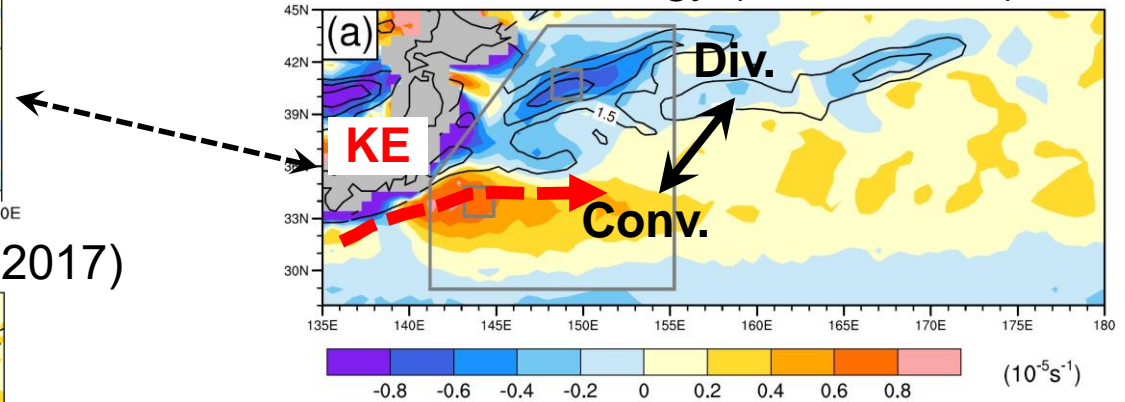
Role of transient eddies in mean surface conv./div. (KOE)

Masunaga, Nakamura, Miyasaka (2019 JC in press)

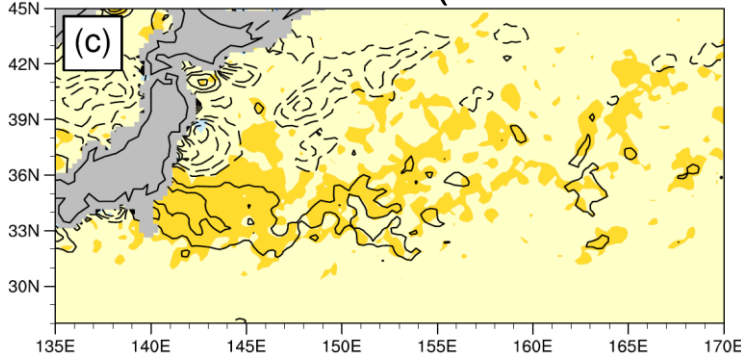
DJF climatology (satellite)



DJF climatology (JRA-55CHS)



extreme transients (O'Neill et al. 2017)

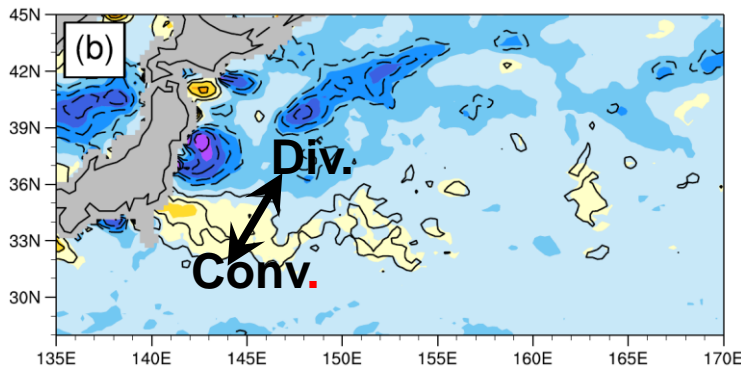


- **JRA-55CHS**: Global atmospheric reanalysis (model resolution: 0.56 deg.)

- MGDSST (0.25 deg. resolution) is prescribed, which can resolve the major WBC structures

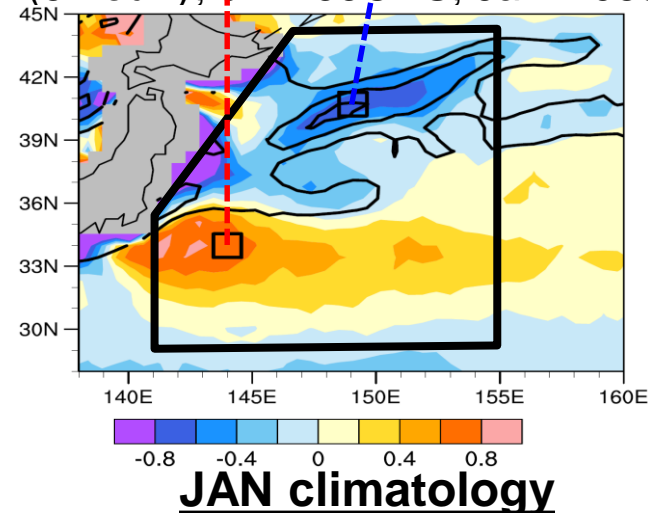
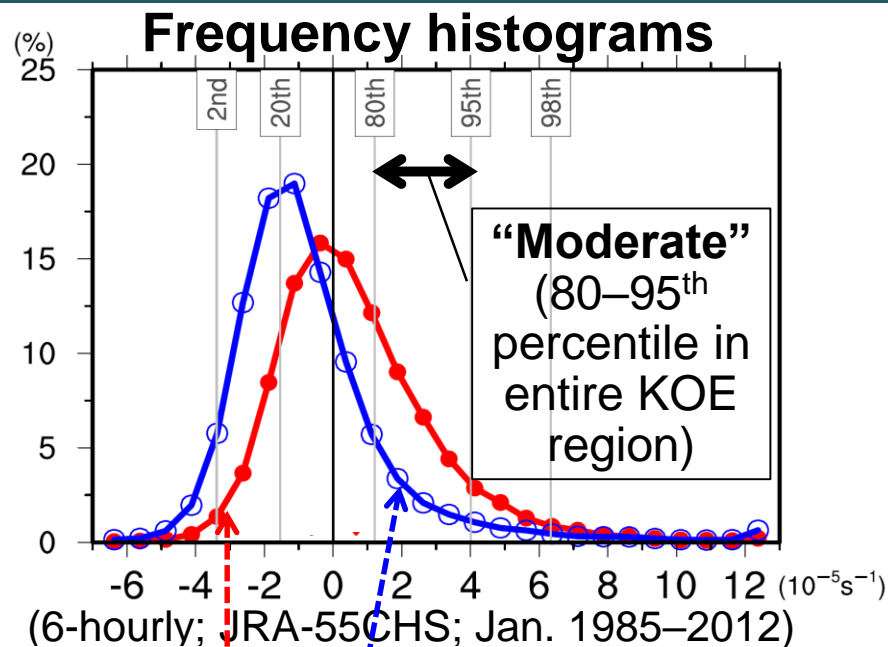
- Climatologies in surface div./conv. in JRA-55CHS are consistent with those in high-resolution satellite observations (Masunaga et al. 2018; SOLA).

Residual: div.-conv. contrast remains

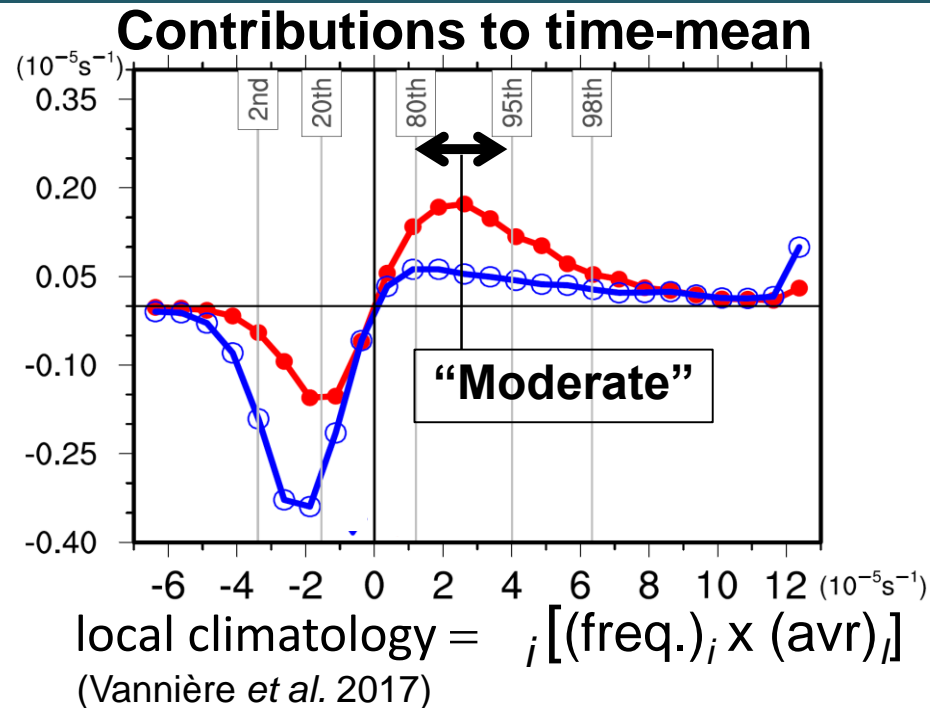


Histograms and contributions of sfc. wind conv. (KOE)

Masunaga, Nakamura, Miyasaka (2019, JC in press)



surface wind **Conv./Div.** (10^{-5} S^{-1})
+ SST gradient

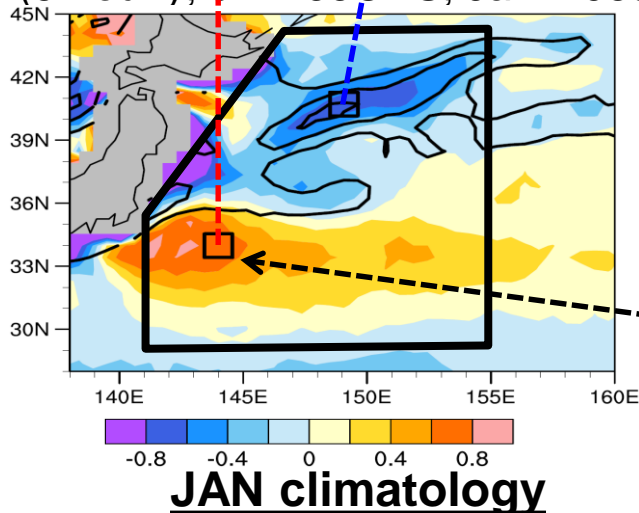
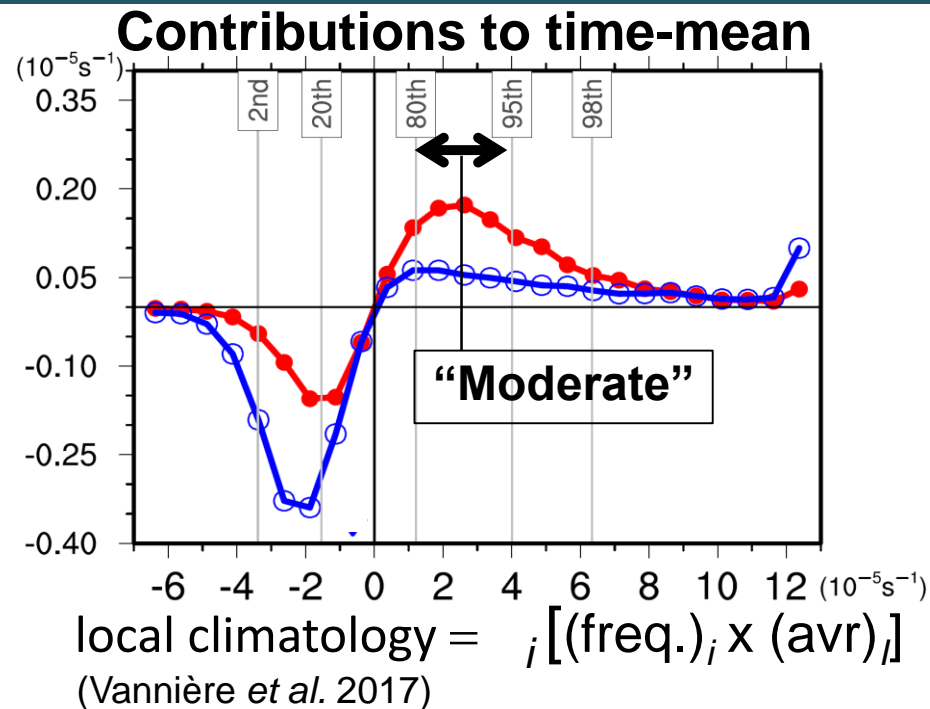
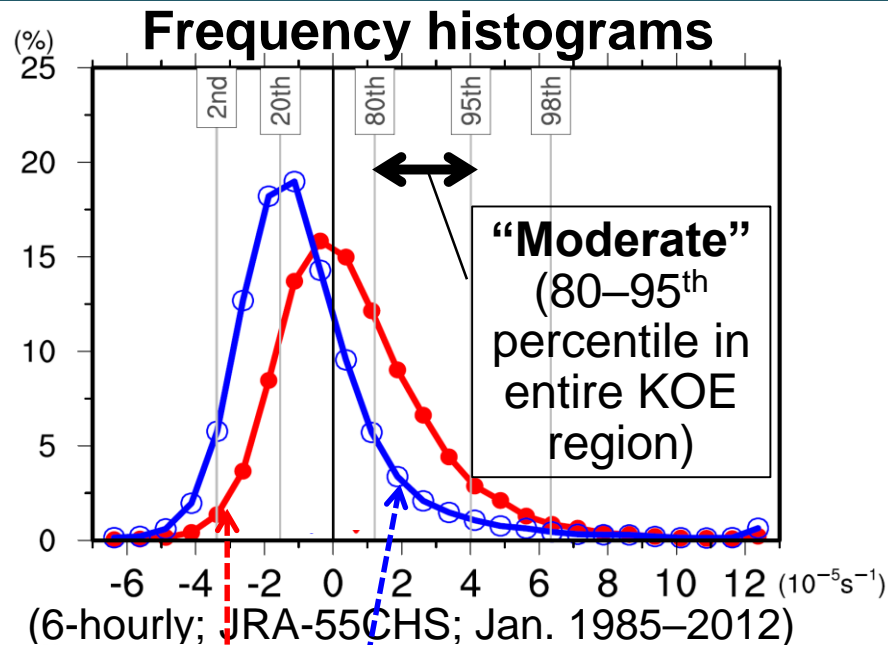


- Virtually **NO** north-south difference in contributions from **extreme conv.** (or div.) to the climatology.
- Climatological **north-south difference** arises mainly from **moderate conv.** (or div.).

KOE: Kuroshio-Oyashio Extension

Histograms and contributions of sfc. wind conv. (KOE)

Masunaga, Nakamura, Miyasaka (2019 JC, in press)



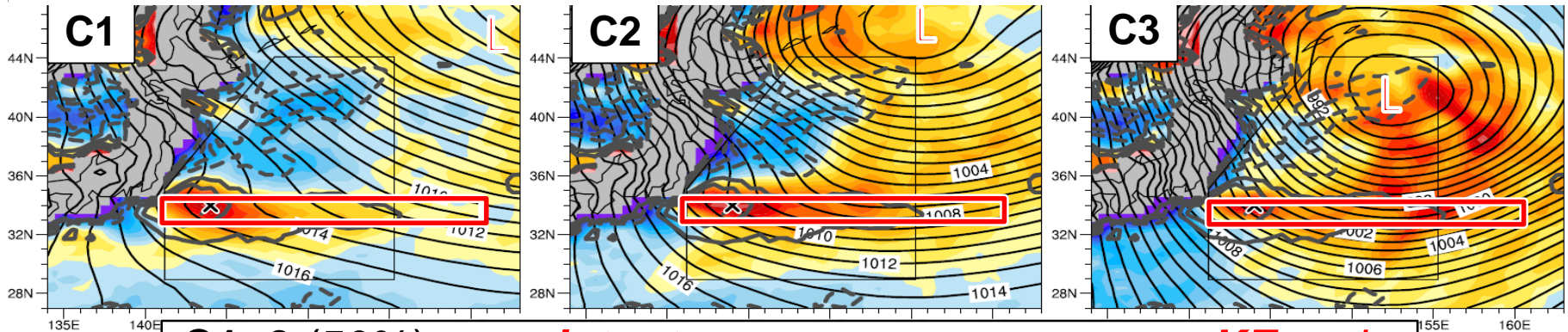
- 900 snapshots of moderate conv. at climatological maximum, where *the histogram is least skewed*.
- Apply cluster analysis to SLP over KOE region to identify typical atmospheric flow patterns inducing moderate conv.

surface wind Conv./Div. (10^{-5} s^{-1})
+ SST gradient

Typical synoptic situations for moderate conv. events

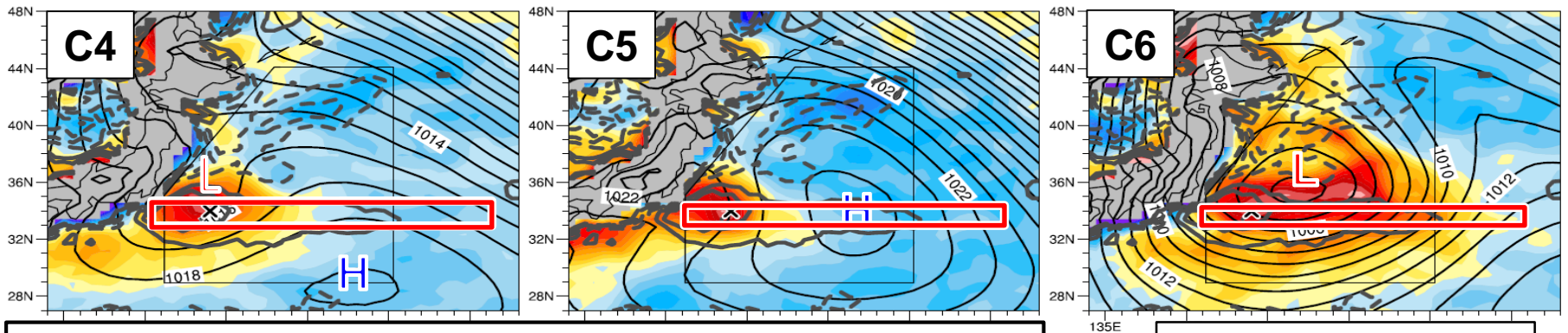
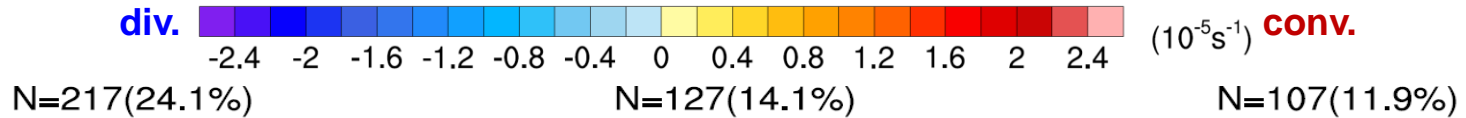
Masunaga, Nakamura, Miyasaka (2019 JC, in press)

→ Convergence over warm KE persists at least for the next 12 hours.



C1~3 (50%): persistent convergence over warm KE under monsoonal northwesterlies behind a developed storm

composited surface wind **div./conv.** vs. its **JAN. climatology**; composited SLP (every 1hPa)

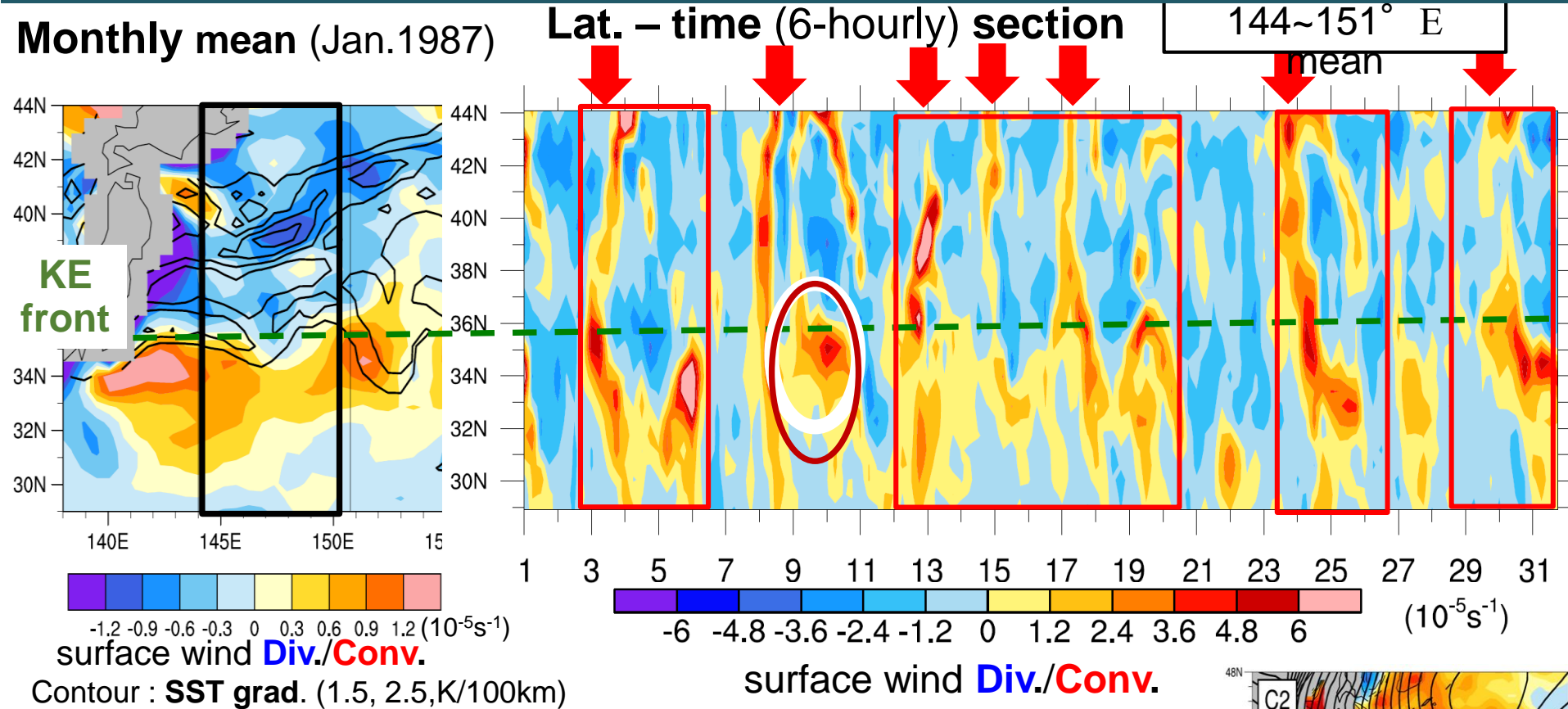


C4-5 (38%): meso- α low/trough over warm KE accompanying southerlies

C6 (12%): synoptic cyclone over KE

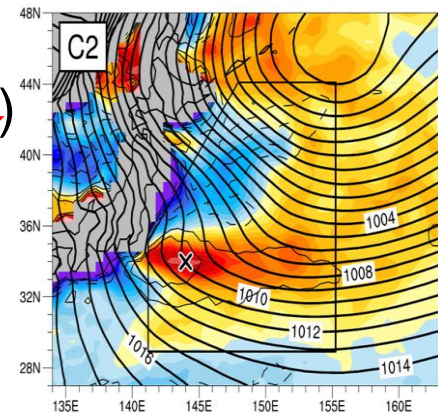
Latitude-time section of surface conv. over KOE (Jan. 1987)

Masunaga, Nakamura, Miyasaka (2019 JC, in press)



- **Strong conv. events associated with synoptic cyclones (↓) are short-lived to the north of the KE front, where divergence is dominant.**

- **After passage of a cyclone, wind convergence tends to persist along the warm KE, as in Cluster C2.**



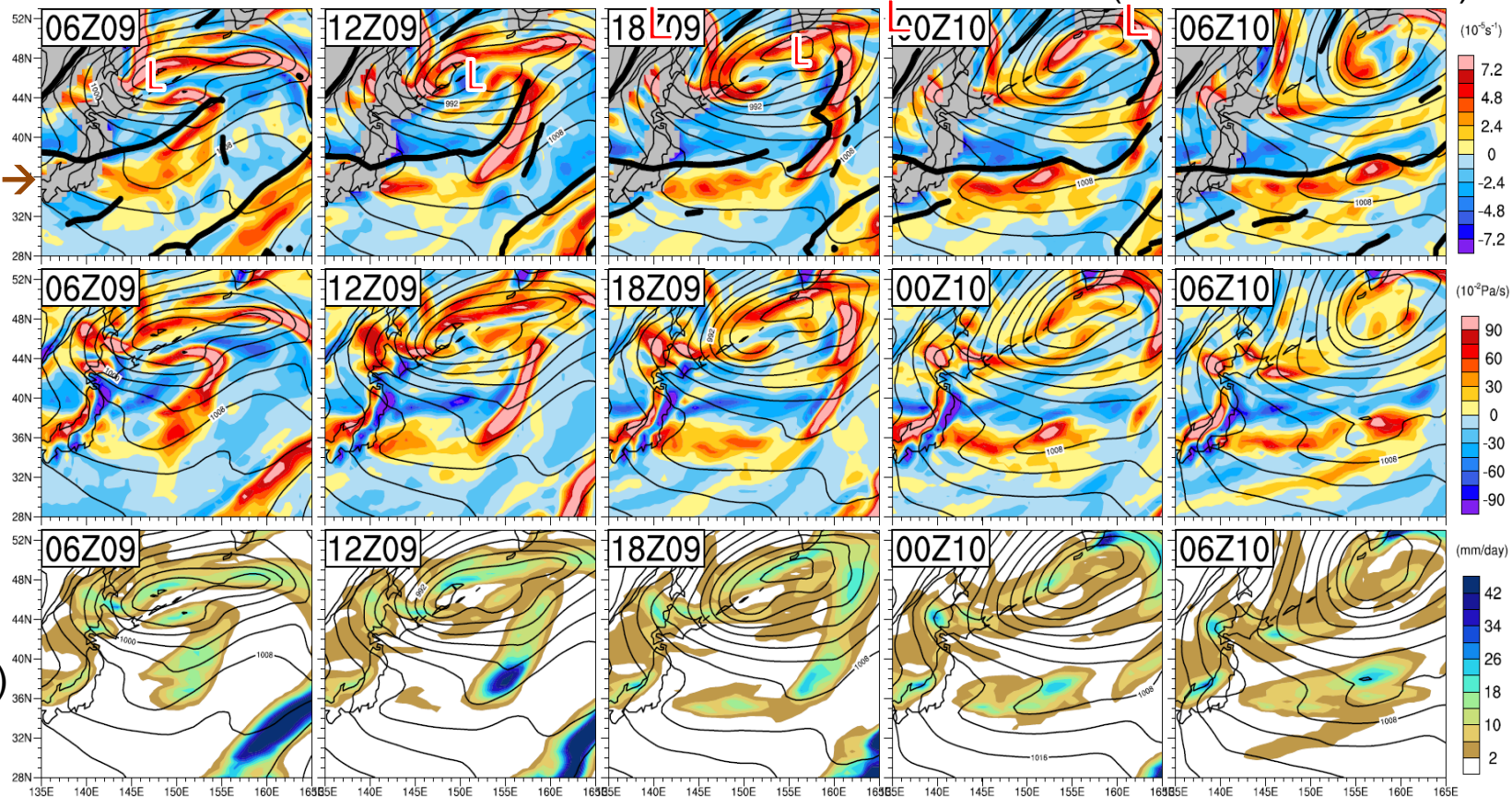
Synoptic situation for moderate conv. event (early Jan. 1987)

Masunaga, Nakamura, Miyasaka (2019 JC, in press)

Heavy solid lines: atmos. fronts detected with “Thermal Frontal Parameter” (Hewson et al. 1998)

surface
conv./div.

SST front →



- After the passage of a cyclone, zonal bands of **surface convergence**, **ascent** and **shallow convective precipitation** are organized along an atmospheric **stationary front anchored by SST front along KE**, as in Cluster 2.
- Similar evolution occurs along the Gulf Stream (c.f. Parfitt % Seo 2018).

Impacts of higher SST resolution on ERA-Interim

Masunaga et al. (2015, 2016 J. Clim.)

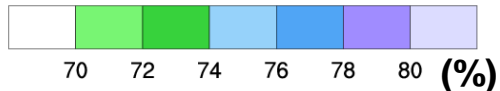
Atmospheric model: TL255
(~ 0.75° grid intervals)

Multiple SST fronts in the KOE
(Kuroshio-Oyashio Extension) region
are resolved in higher-resolution
SST prescribed since 2002.

shade: | SST / y |, contour: SST

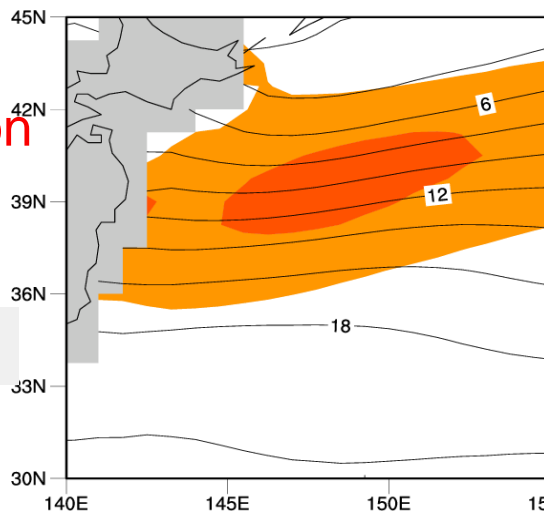


shade: climatological cloudiness

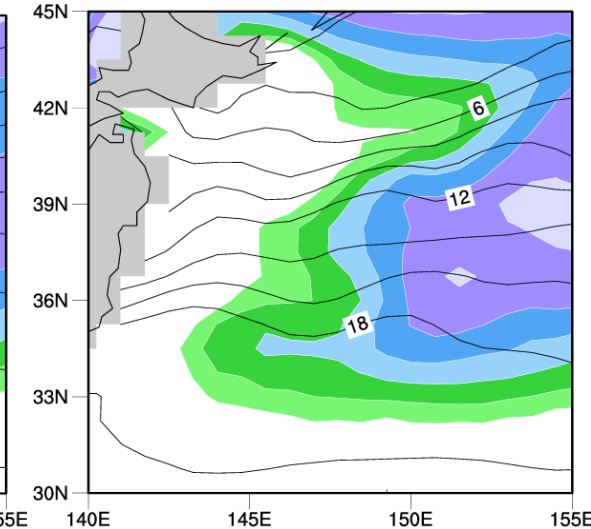
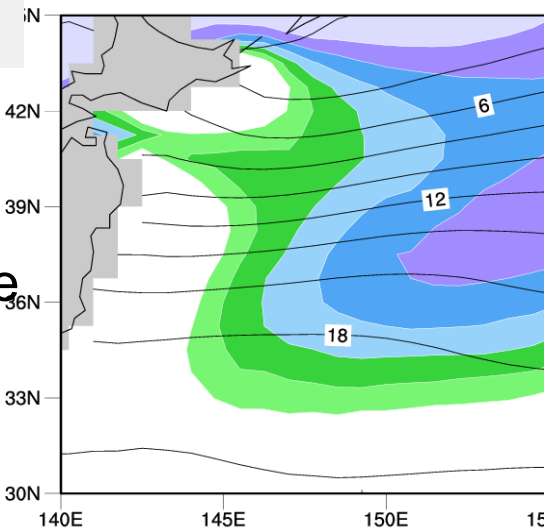
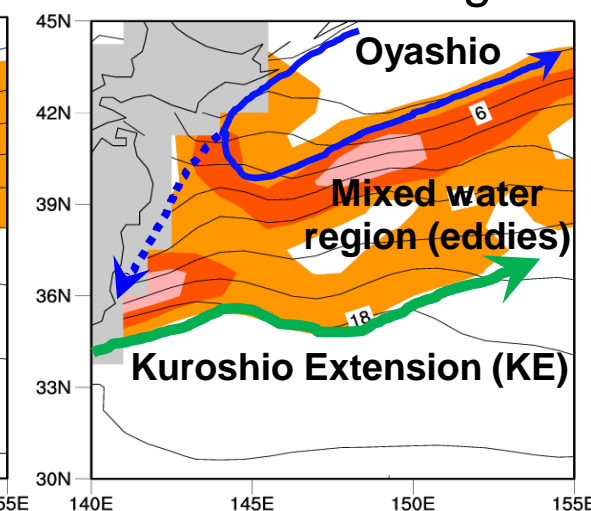


Improved representation of
“mesoscale” structures in surface
wind, **cloudiness**, precipitation,
with higher consistency with
satellite observations.

1979–2001 (DJF)
SST res.: 1.0°



2002–2012 (DJF)
SST res.: 0.5° or higher



c.f. Parfitt et al. (2017) for GS

JRA-55CHS as a new member of JRA-55 family

Horizontal resolution: TL319 (~55km) with 60 vertical levels (top:01hPa)

	JRA-55 (Main product)	JRA-55C (Conventional)	JRA-55CHS (High-res. SST)
SST	COBE-SST (1°)	COBE-SST (1°)	MGDSST(0.25°)
assimilated atmos. data (4-D Var.)	All (in-situ + satellite)	In-situ only	In-situ only
period	1958~ current	1958~2012	1982~2012
	Kobayashi et al. (2015 JMSJ)	Kobayashi et al. (2014 SOLA)	Masunaga et al. (2018 SOLA)

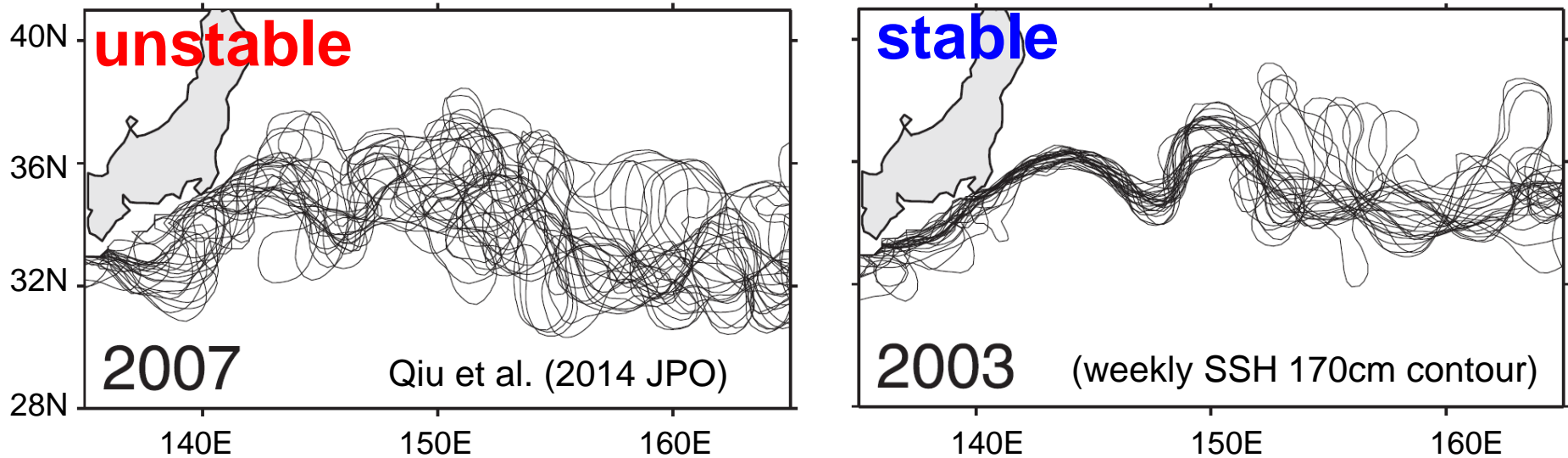
JRA-55CHS:

Additional JRA-55 product produced jointly by MRI (JMA) and "HotSpot project" (2010-2015; lead PI: H. Nakamura)

Purpose: Assessing the significance of SST resolution on global atmospheric reanalysis through comparison among JRA-55 family, ERA-I and satellite observations

Local atmospheric response to two dynamical regimes of KE

Masunaga et al. (2016 JC, 2018 SOLA)



- KE fluctuates between stable and unstable regimes on decadal scales.
- **More warm-core eddies** are shed from unstable KE (Sugimoto et al. 2011)
 - **warm SST anomalies** to the north of mean KE axis
- Satellite obs. capture associated persistent imprints as atmospheric mesoscale variations (Masunaga et al. 2016).

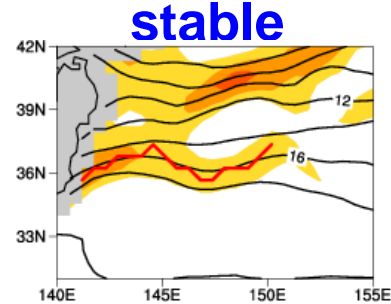
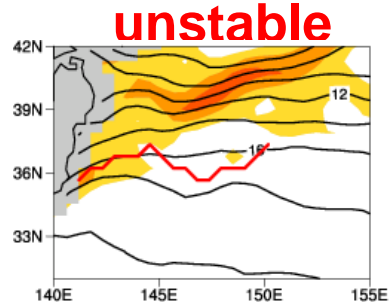
c.f. Révelard et al. (2017) for large-scale response

Purpose: Assessing performances of atmos. reanalysis in representing atmospheric imprints of the KE variability in winter

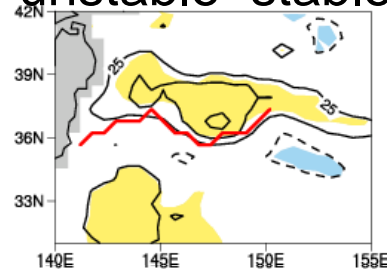
SST, $|dSST/dy|$ composited for stable/unstable KE regimes

Masunaga et al. (2016 JC, 2018 SOLA)

JRA-55CHS
(1989-2012)

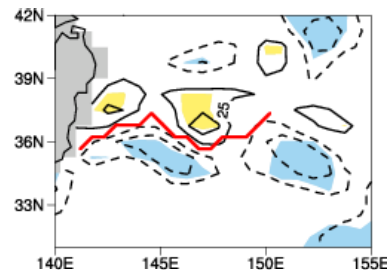
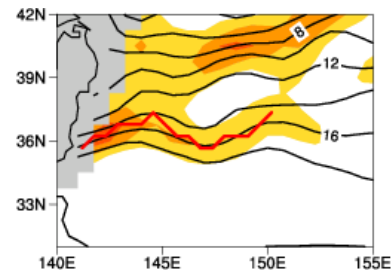
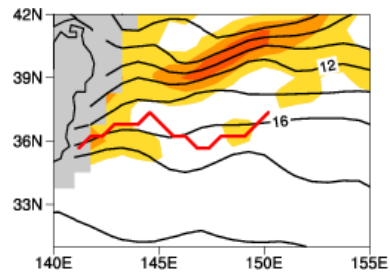


unstable-stable (LHF+SHF, SST)



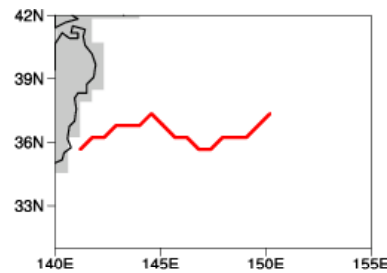
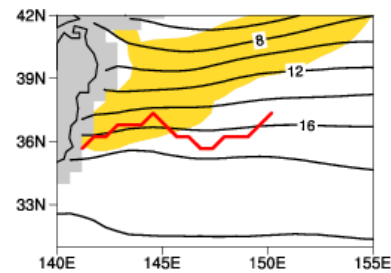
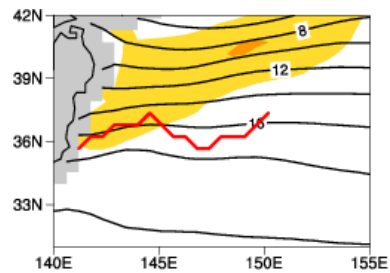
Heat fluxes from the ocean increase over warm SST anomalies due to active warm-core eddies.

ERA-I
(2002-2012)



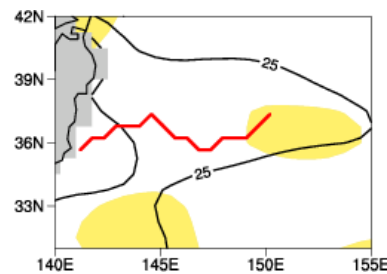
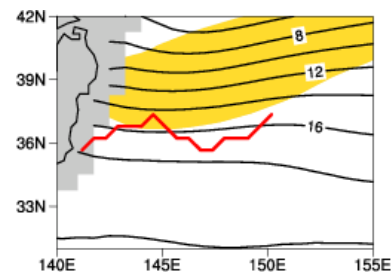
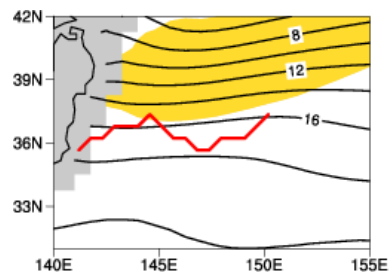
(pos. cor. between SST and SHF/LHF)

JRA-55C
(1989-2012)



Anomalies are diminished.

ERA-I
(1989-2001)



shade:90% significance

Anomalous surface wind conv. associated with KE variability

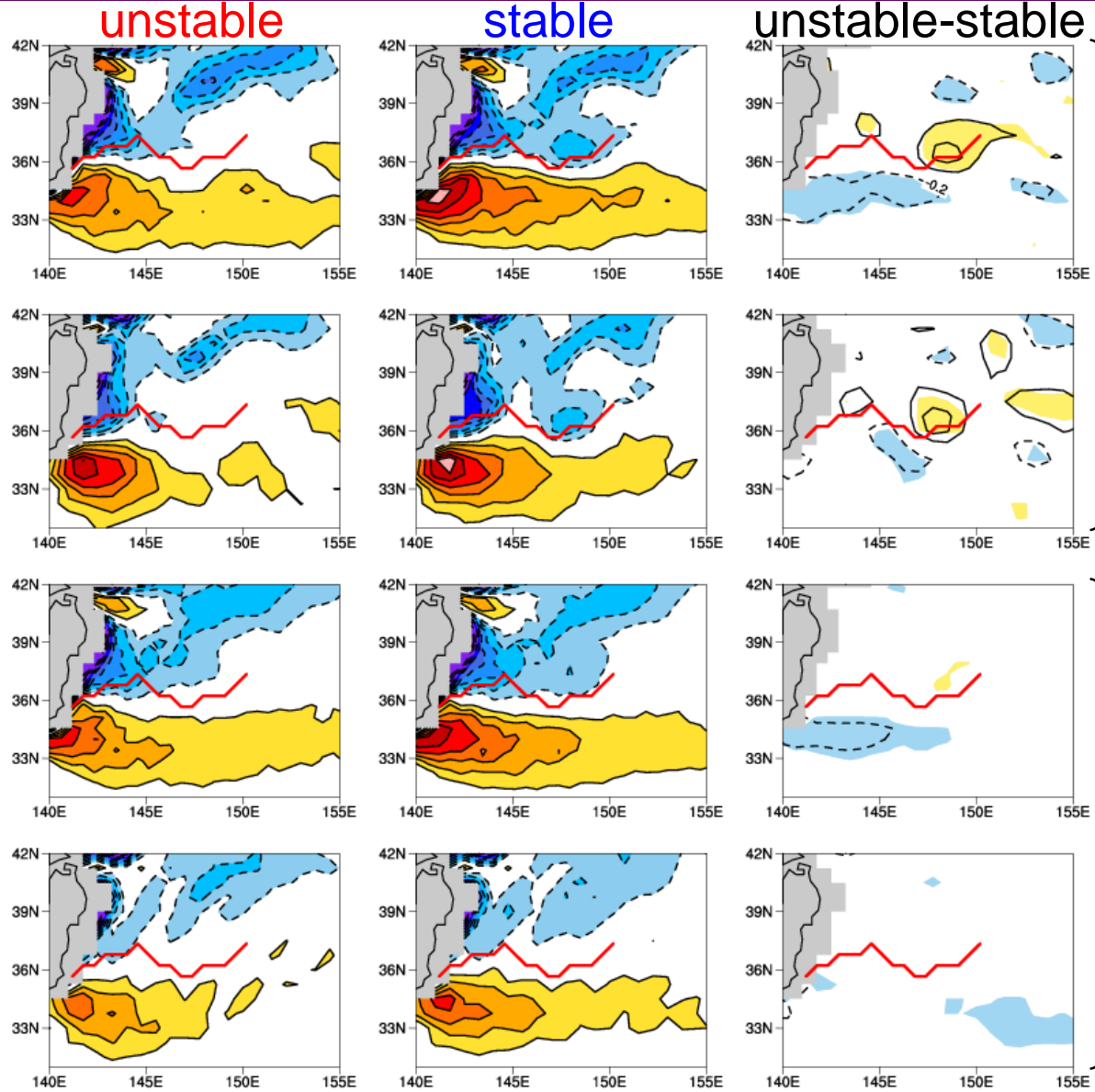
Masunaga et al. (2016 JC, 2018 SOLA)

JRA-55CHS
(1989-2012)

ERA-I
(2002-2012)

JRA-55C
(1989-2012)

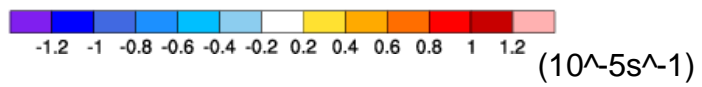
ERA-I
(1989-2001)



Anomalous conv.
over warm SST
anomalies

Diminished signal
as an
atmospheric
response to KE
variability.

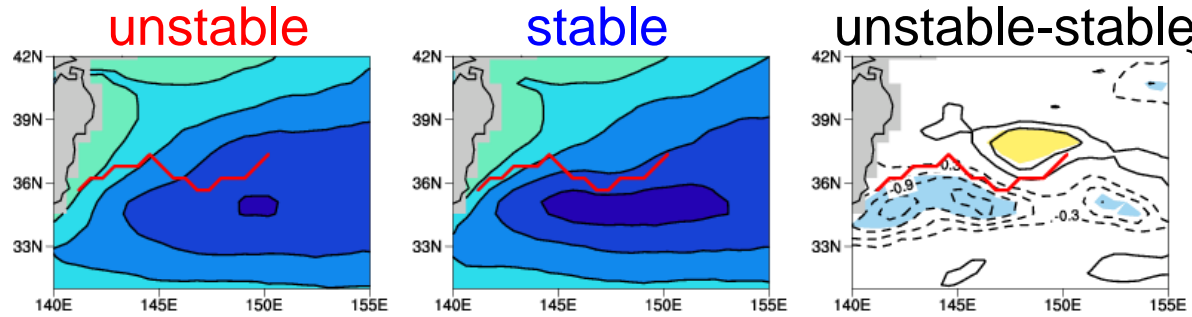
shade:90% significant



Anomalous precipitation associated with KE variability

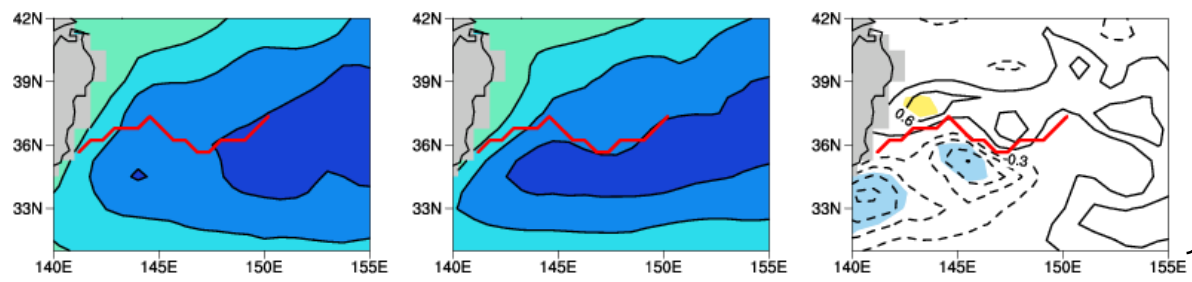
Masunaga et al. (2016 JC, 2018 SOLA)

JRA-55CHS
(1989-2012)

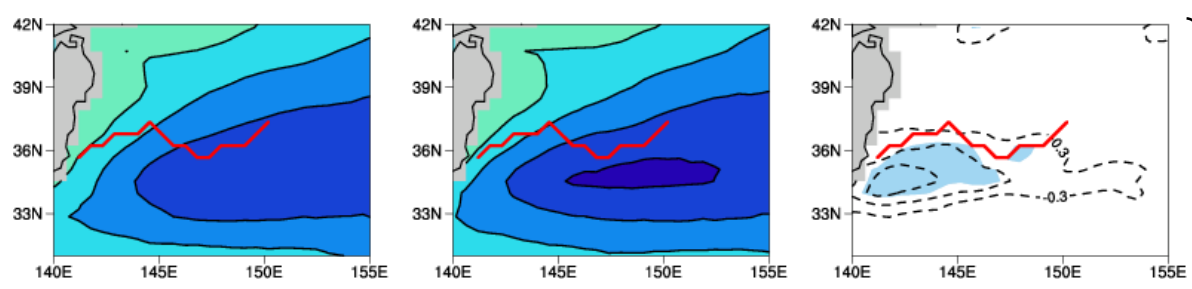


Anomalous increase in total precipitation over warm SST anomalies

ERA-I
(2002-2012)

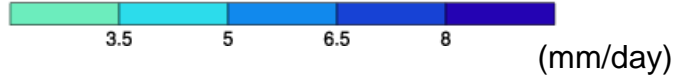
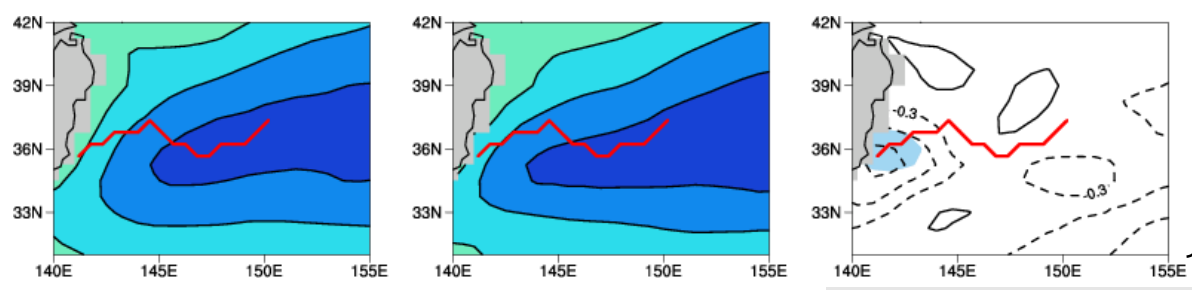


JRA-55C
(1989-2012)



Diminished signal as an atmospheric response to KE variability.

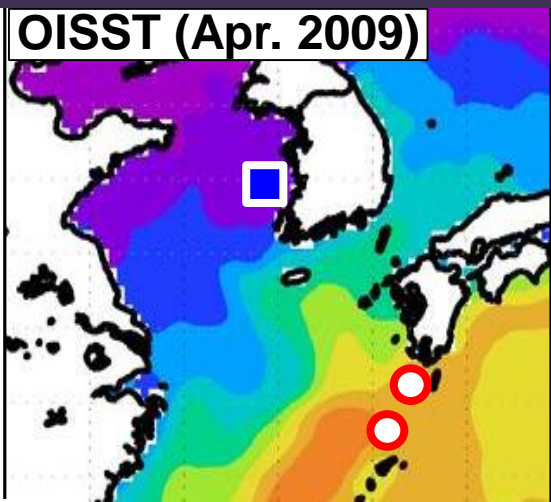
ERA-I
(1989-2001)



shade:90% significant

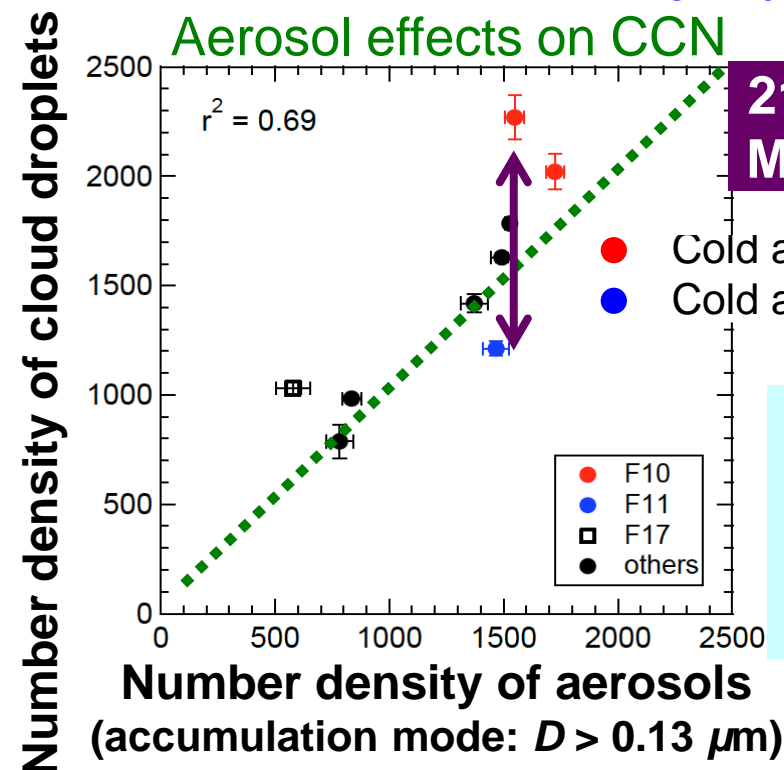
Cloud microphysics modulated by the warm Kuroshio

Koike et al. (2012 JGR; 2016 JGR)

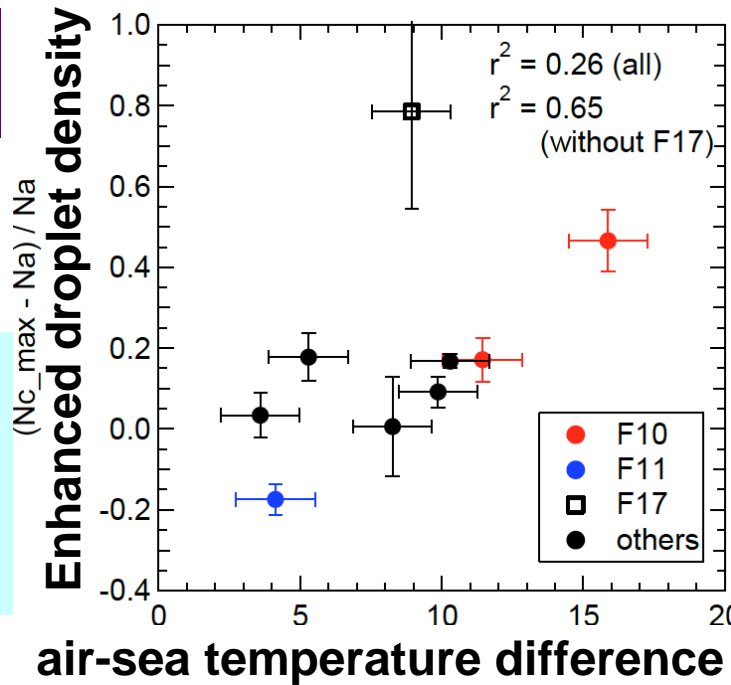
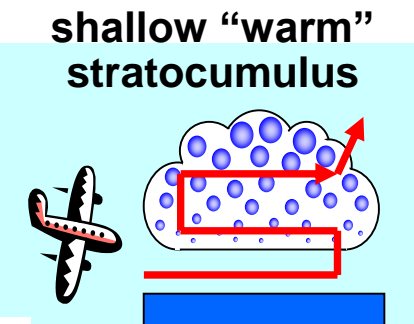


Cold-air outbreak from the continent onto the Kuroshio

- reduced stratification
- enhanced updraft [0.4 → 1.2 m/s]
- enhanced associated adiabatic cooling
- higher super-saturation level
- activation of smaller aerosols as CCN
- **higher cloud albedo** [fractional increase: 11%]
- **enhanced cloud radiative forcing** [-4.7 W/m²]

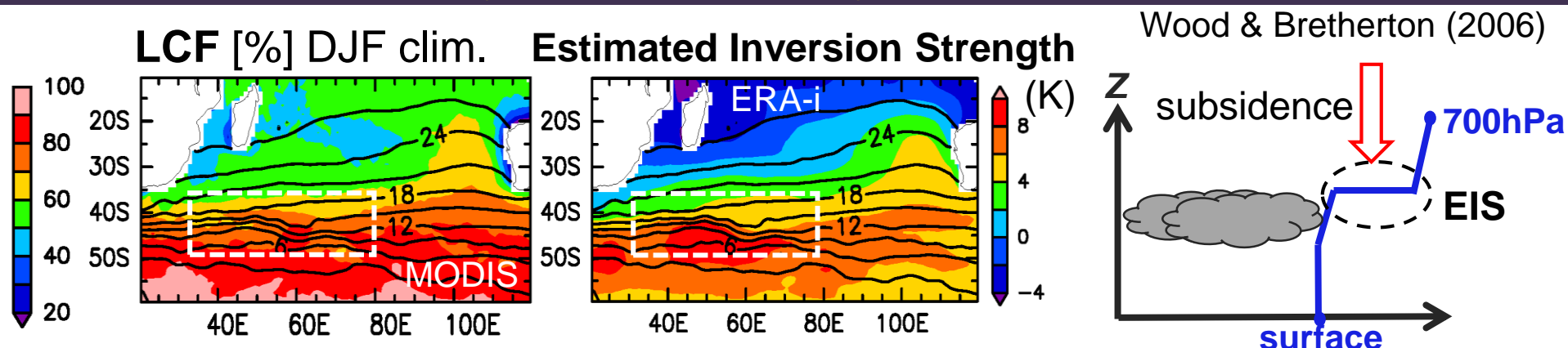


21 flights during Mar. 26 ~ Apr. 25



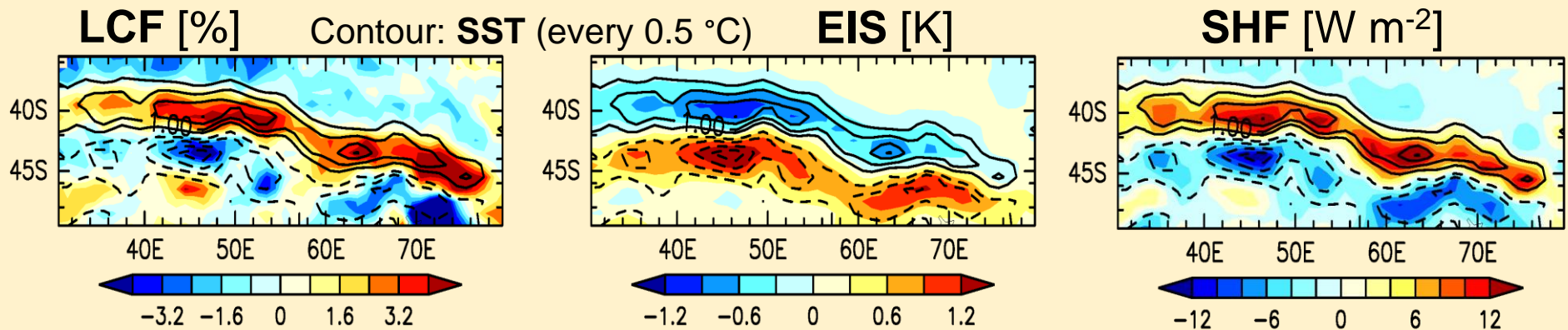
Low-Cloud Fraction (LCF) contrast across Agulhas SST front

Miyamoto, Nakamura, Miyasaka (2018JC)



EIS can overall explain the distribution of LCF (Wood & Bretherton, 2006; Wood 2012).

✓ Latitudinal 9° high-pass filtering for highlighting impacts of the Agulhas SST front



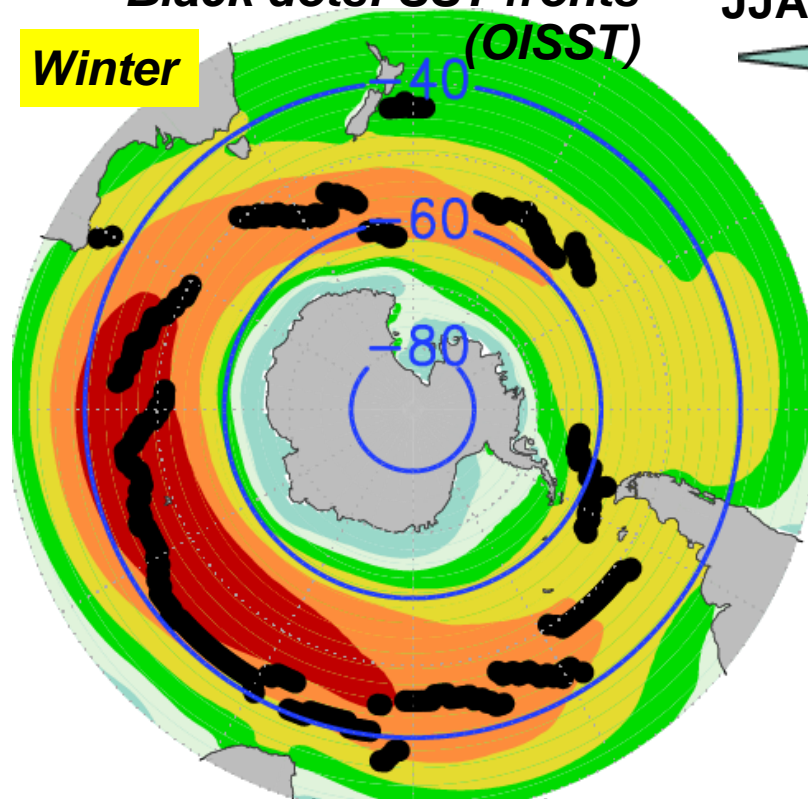
- **Local LCF maxima along the warm Agulhas Return Current**
- This LCF maxima cannot explained by EIS minima (= reduced stratification) over warmer water, but rather **enhanced SHF acts to destabilize MABL and thus increase LCF over the warm Agulhas Current with higher CCN, LWP and optical thickness** (Koike et al. 2012, 2016).

Collocation of low-level westerlies with SH SST fronts

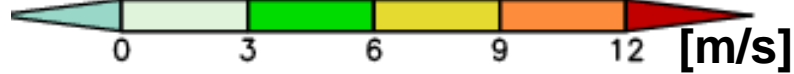
Nakamura, Shimpo (2004 J.Clim.); Nakamura et al. (2008 GRL)

Black dots: SST fronts
(OISST)

Winter



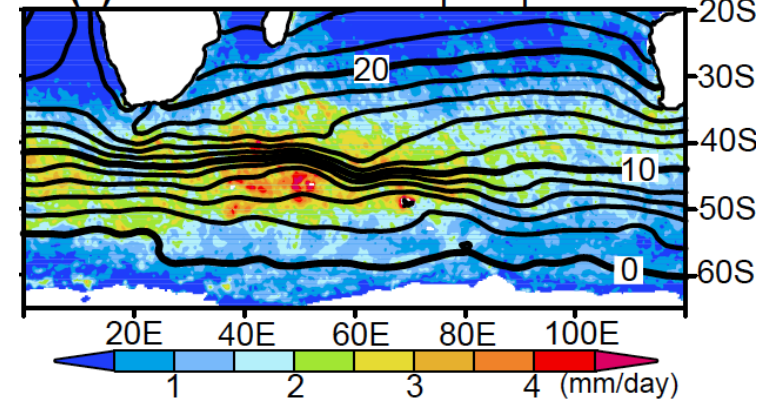
JJA climatology of 925hPa westerlies (U925)



- Overall latitudinal correspondence between SST fronts and U925 axis
- **SST front** can efficiently maintain a surface baroclinic zone against eddy heat transport, which is necessary for recurrent cyclone development and thereby the formation of a stormtrack and eddy-driven polar-front jet (PFJ).

JJA climatology for the S. Indian ocean

(a) SST with AMSR-E precipitation



ERA-Interim (1979-2011)

- Moisture supply from warm currents also contributes to storm development.
- Frontal SST gradient can be important for the annular mode as wobble of PFJ.

(Nakamura et al. 2008 GRL; Sampe et al. 2013

JMS.J)

"Aqua-planet" AGCM experiments (T79 L56)

Ogawa, Nakamura et al. (2012 GRL; 2016 JC)

- AGCM for Earth Simulator (AFES)
T79 (~150km), 56 levels
- "Aqua-planet" experiments with zonally uniform SST with no landmass
- perpetual **winter** integrations for 120 months

Control (CTL) experiment

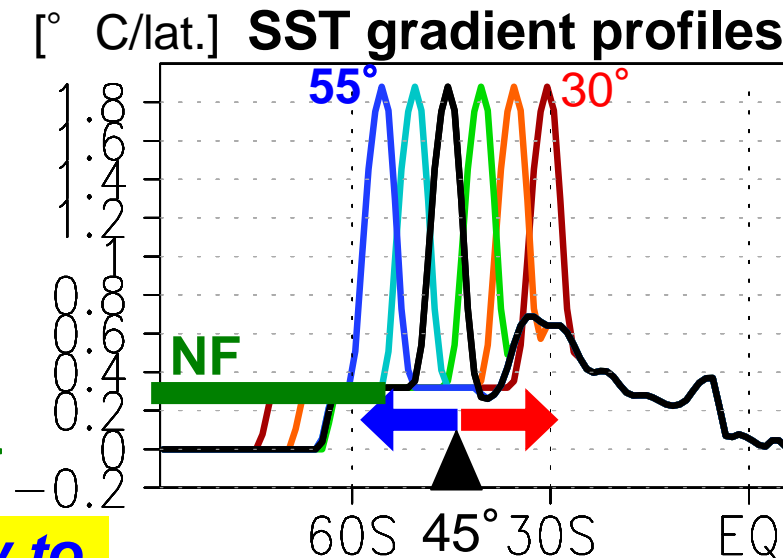
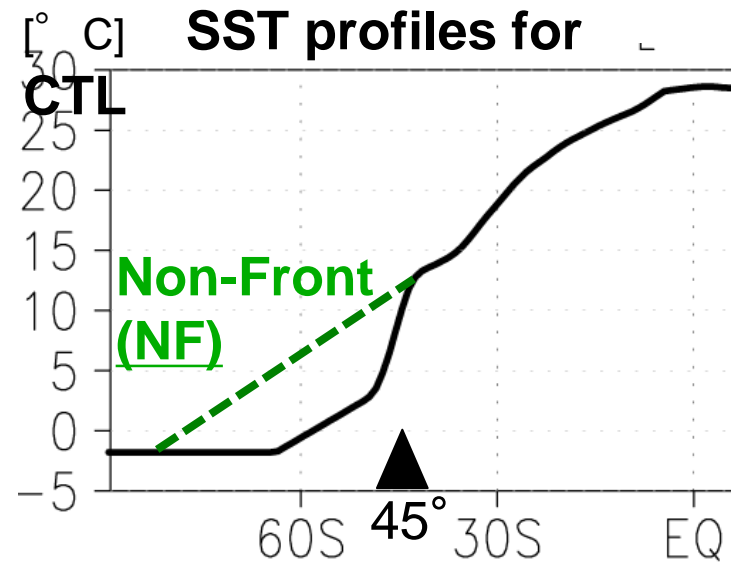
JJA OI-SST profile for the South Indian Ocean, characterized by SST front at 45° S.

Sensitivity experiments

SST front is **shifted from 30° S to 55° S** with 5° intervals, while its intensity is fixed.

Non-front (NF) experiment

Frontal SST gradient eliminated (no ACC).



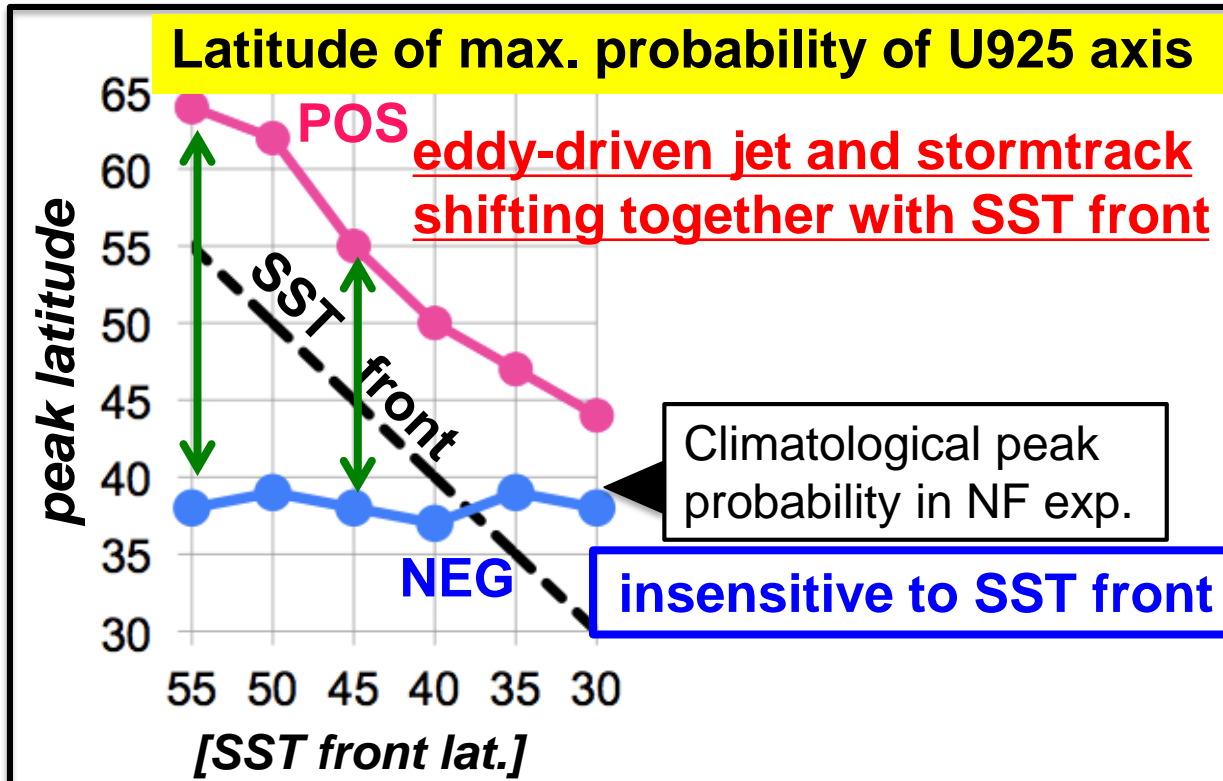
No SST changes in the tropics/subtropics!

→ Sensitivity of annular mode variability to the latitude of SST front is investigated.

“Regime-like” behavior of the model annular mode

Ogawa, Nakamura et al. (2016 JC)

- Westerlies composited for POS and NEG exhibit regime-like behavior, indicated as **dual peaks** in probability of surface westerly (U925) axis.



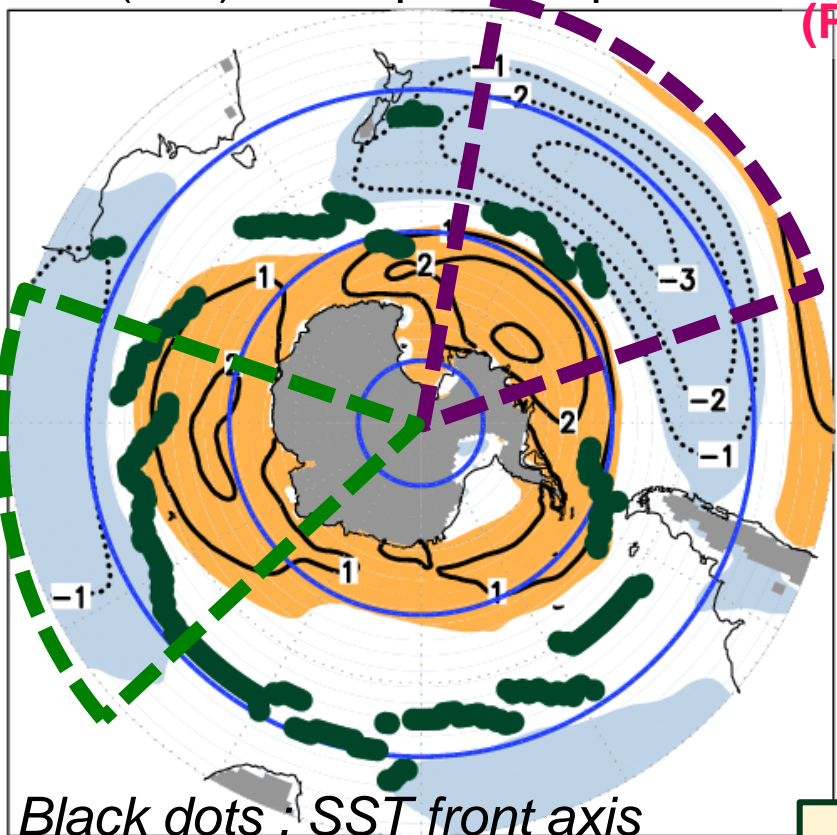
Increasing meridional excursion of PFJ axis with SST front latitude

Annular mode represents wobble between two PFJ regimes, one **forced by frontal SST gradient** and the other **controlled by internal dynamics**.

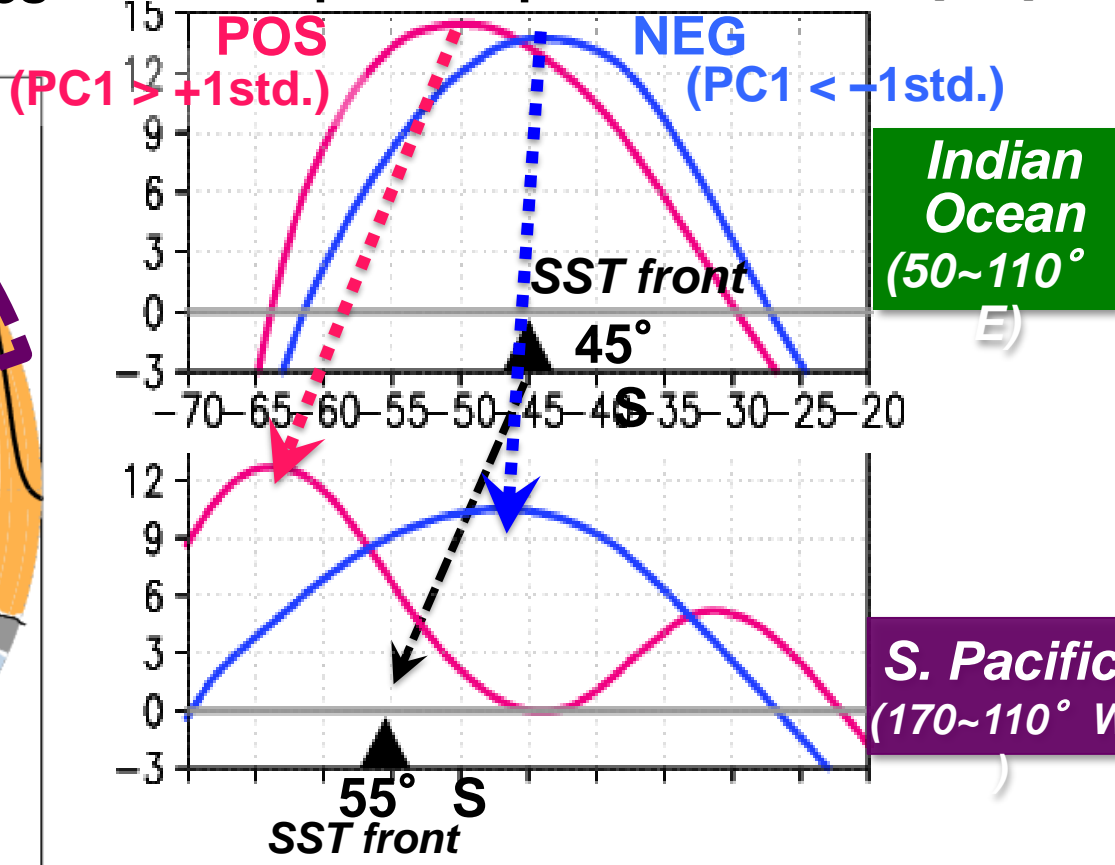
Interpretation of inter-basin differences **observed** in the wintertime SAM signature

Ogawa, Nakamura et al. (JC2016)

SAM-associated U925 anomalies (m/s) in the positive phase



composited profiles of U925 [m/s]



Nakamura's talk in Clim. Var. 10.3 this afternoon (4:30PM)

• **POS: Westerly axis shifts by ~10° corresponding** to the shift of SST front.

• **NEG: Westerly axis stays around 45° S.**

Simulated SAM response to the ozone depletion

Ogawa et al. (2015 GRL)

31-day running mean of zonal-mean westerly response

[m/s]

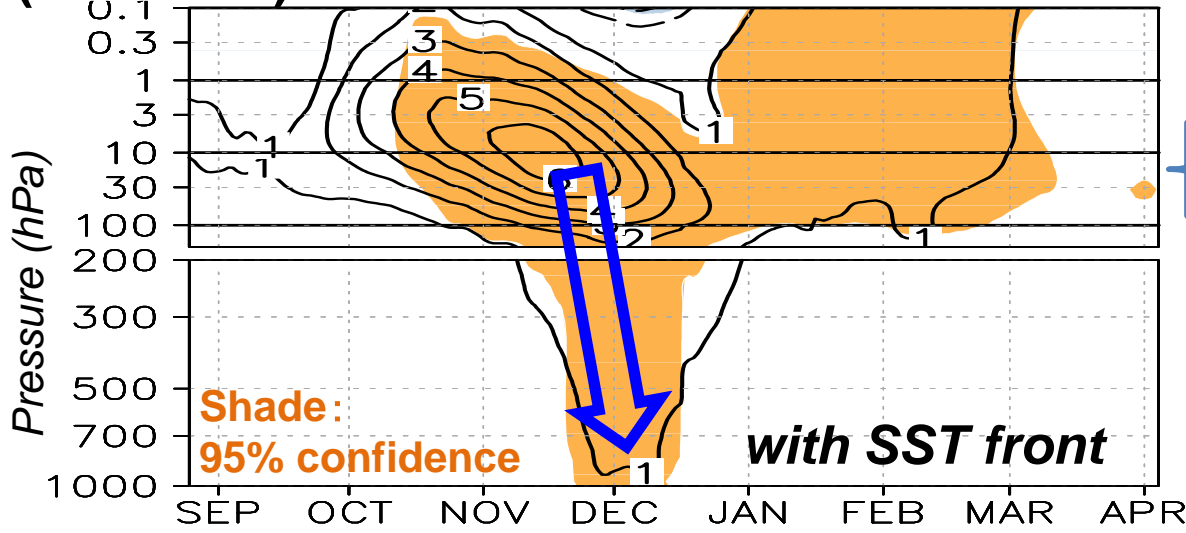
(45~60° S)

Low O₃ – High O₃ (ECHAM5)

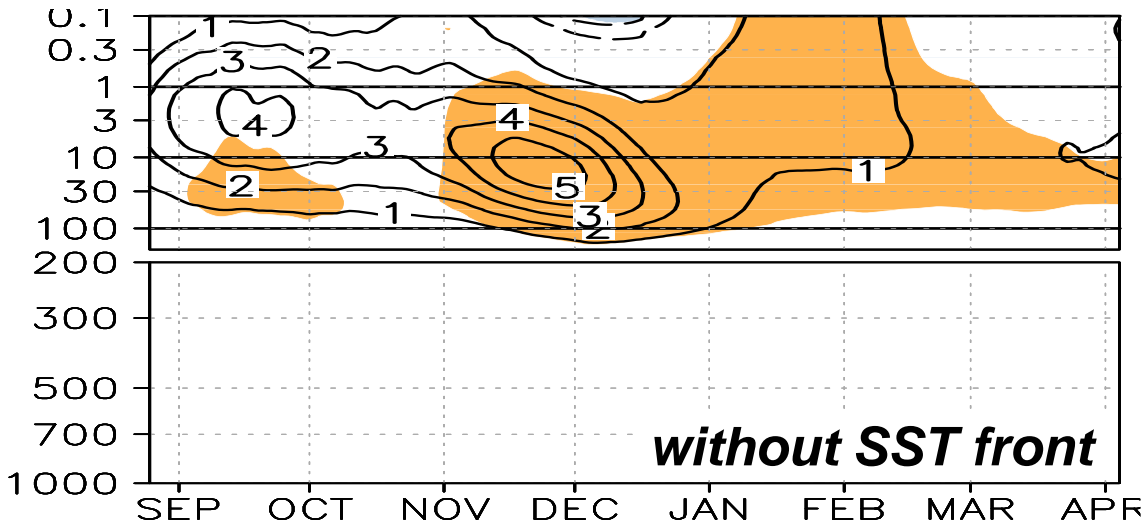
positive values for

polar vortex intensification

positive SAM

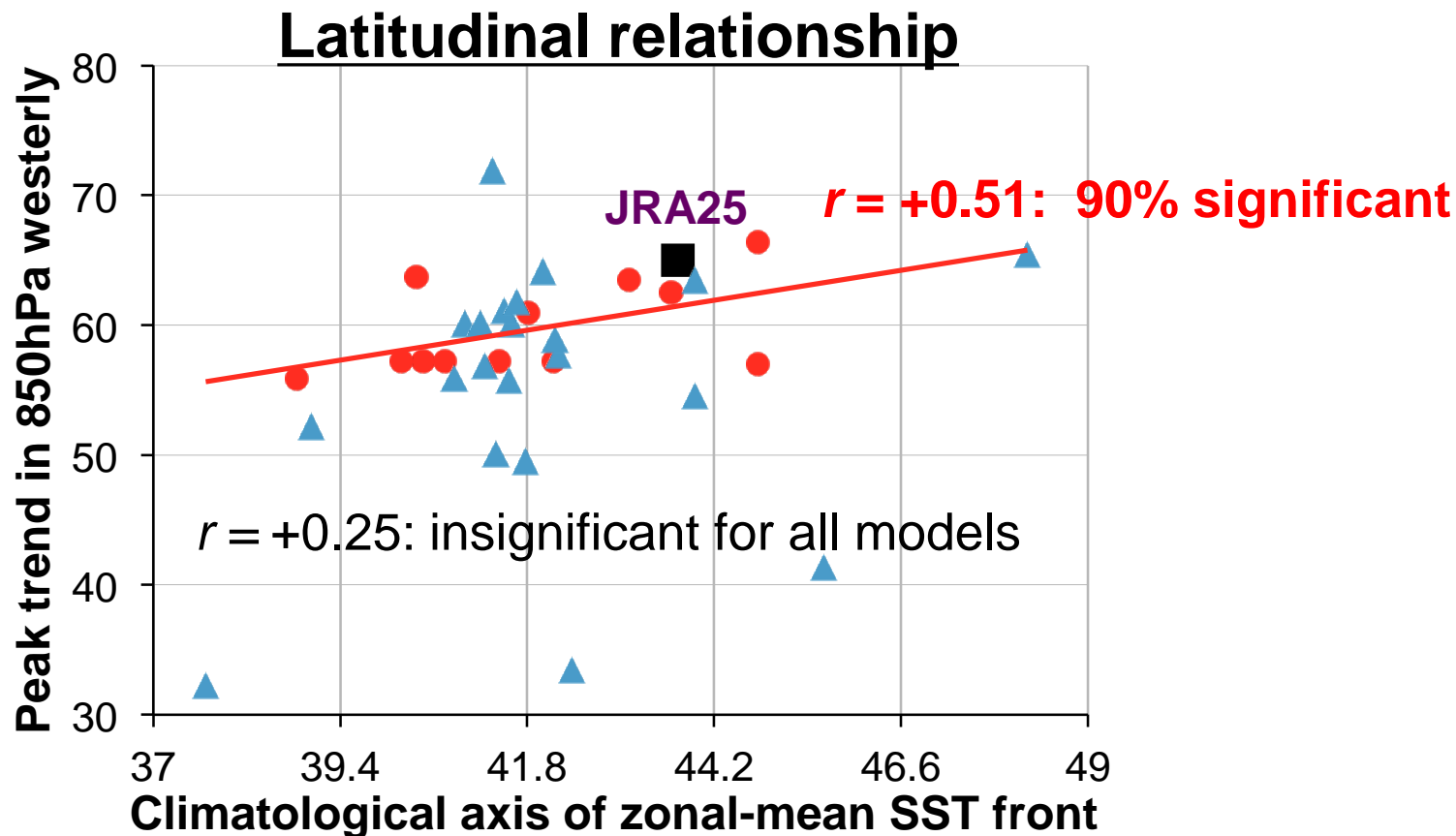


The positive tropospheric SAM trend in summer is reproduced as observed in the presence of frontal SST gradient but not without it.



Westerly trend and SST front simulated in CMIP 3/5 models

Ogawa et al. (2015 GRL)



Among all the models showing stratospheric cooling over Antarctica in late 20c

Red dots: models with stronger SST gradient than reanalysis (+JRA25)

Blue triangles: models with weaker SST gradient

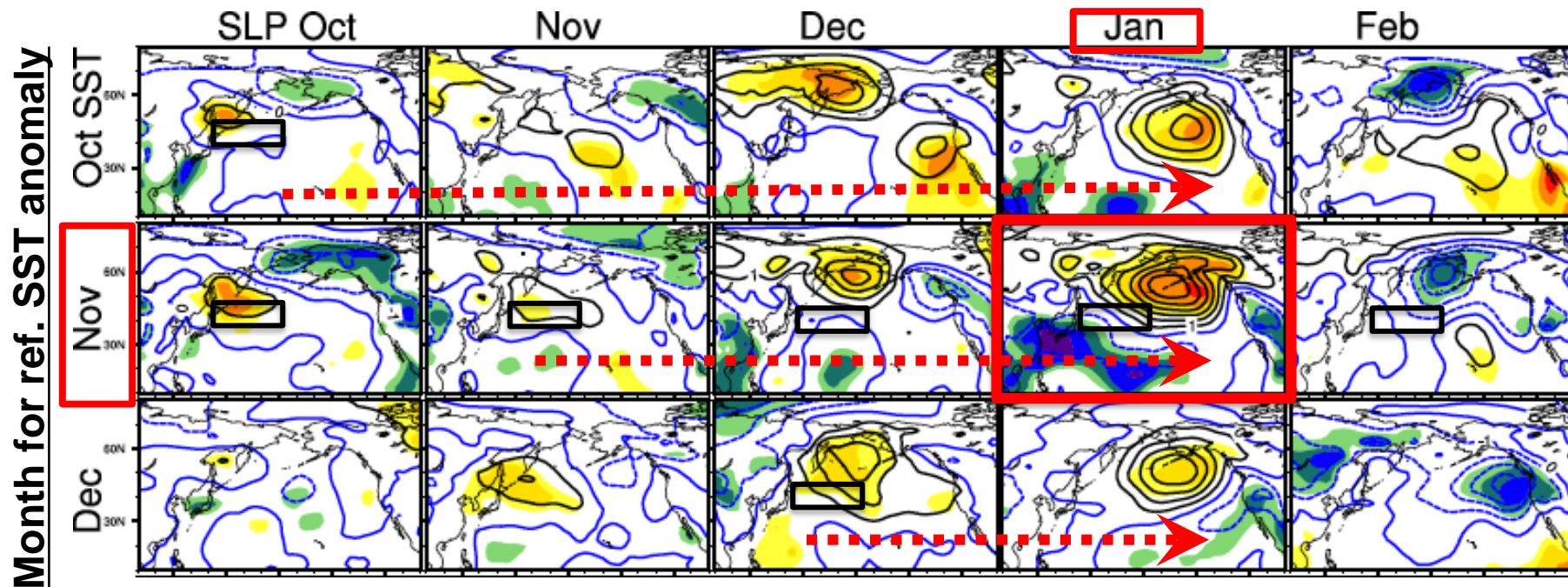
- Reproducibility of the SAM trend in a CMIP model depends on that of SST fronts over the Southern Ocean.

Large-scale atmospheric anomalies forced by decadal SST anomalies in the N. Pacific subarctic frontal zone

Taguchi, Nakamura et al. (2012 J. Clim.)

- Signal of the anomalous Aleutian Low (and PNA pattern aloft) observed **as a response to fall-early winter SST anomalies in the subarctic frontal zone** tends to be strongest in January but break down rapidly into February.
- **Same seasonality is reproduced in 100-yr integration of coupled model CFES.**
c.f. For KE variability: Frankignoul et al. (2011 JC), Révelard et al. (2016 JC)

Monthly evolution of SLP anomalies

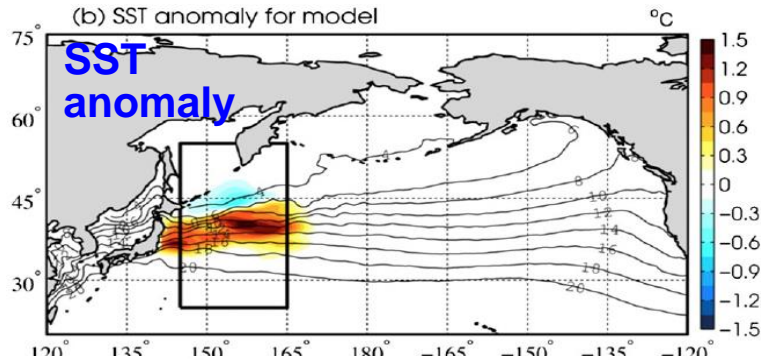


Need for high-resolution modeling (I): more than the “signal to noise paradox”?

(Smirnov et al. 2015 JC)

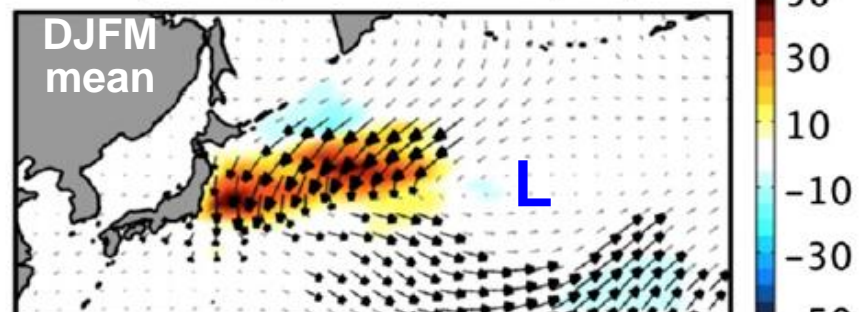
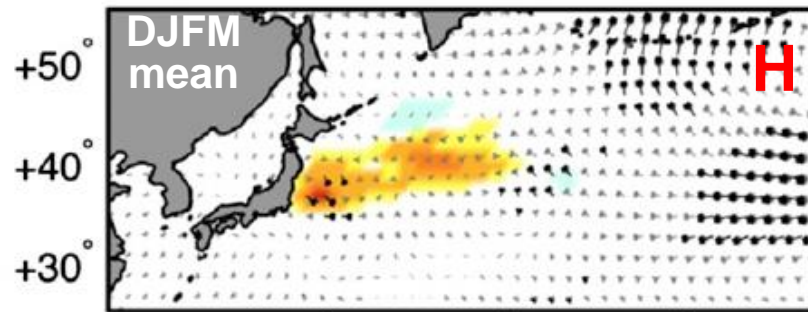
CAM5 0.25° (HR) vs 1° (LR), 25 members

- **HR model simulates a realistic response**, while LR model response is unrealistic.
 - HR model shows higher sensitivity of **convective rainfall** to SST
- ➔ **realistic response in stormtrack activity**



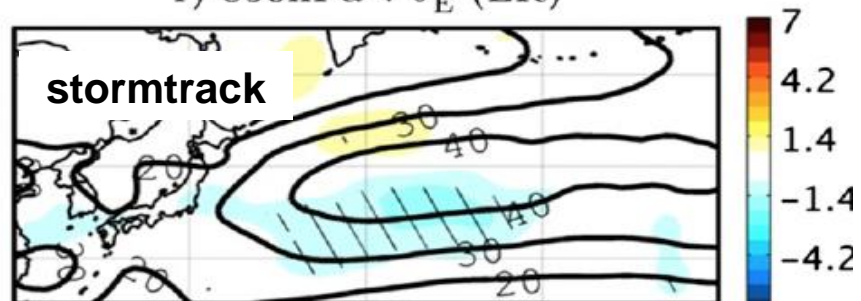
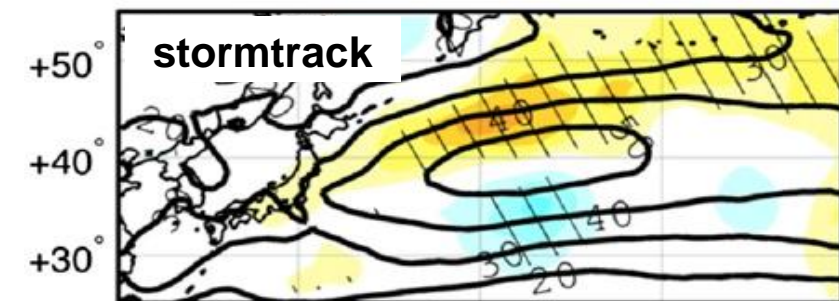
a) THF, 950mb wind (HR)

b) THF, 950mb wind (LR)



e) 850hPa $\overline{v'\theta'_E}$ (HR)

f) 850hPa $\overline{v'\theta'_E}$ (LR)



+140° +160° +180°

H. Nakamura

+140° +160° +180°

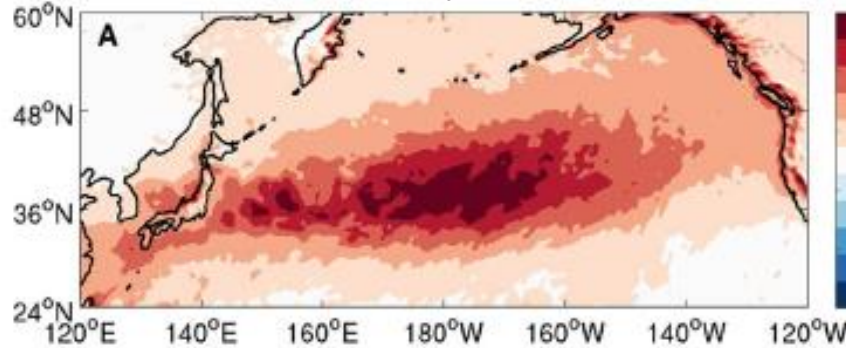
Need for high-resolution modeling (II)

(Ma et al. 2015, 2016)

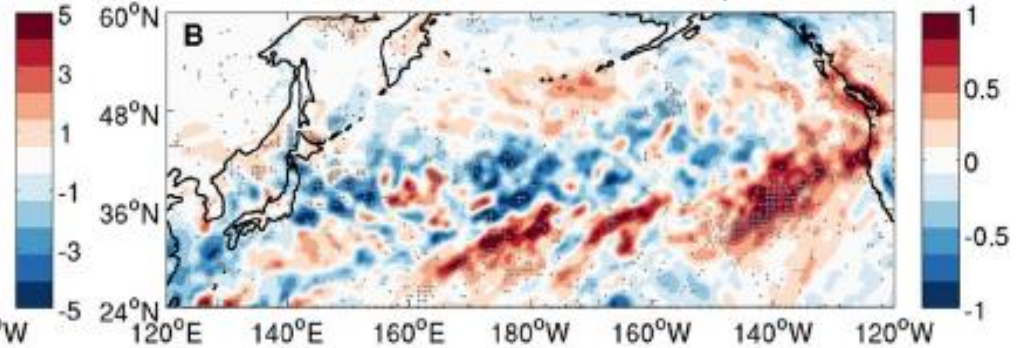
Importance of ocean meso-scale eddies to moist development of storms

vertically integrated diabatic heating with storms (27km model)

with ocean eddy contribution

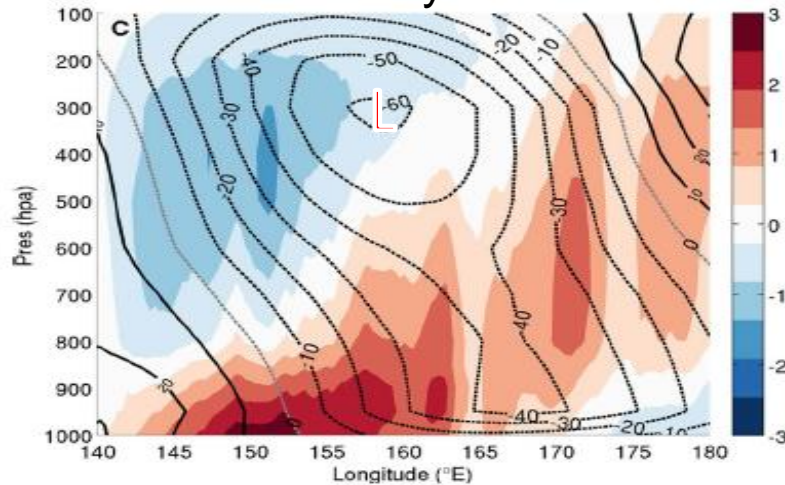


reduction due to suppressed eddy contribution

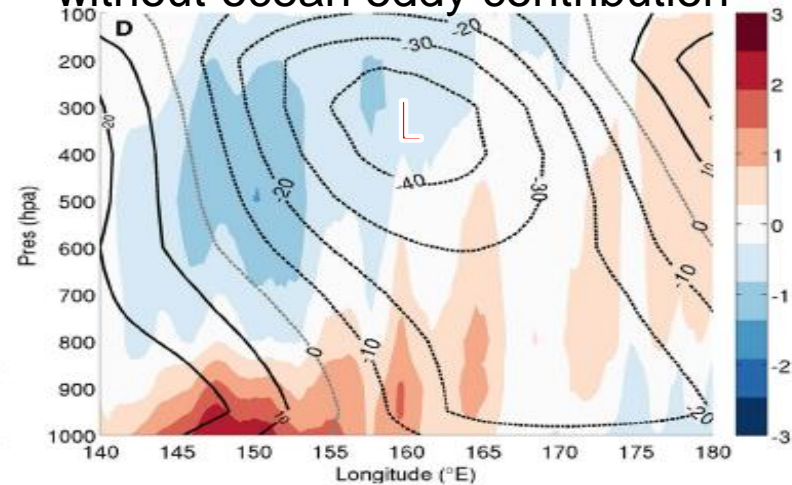


typical cyclone structure with diabatic heating

with ocean eddy contribution



without ocean eddy contribution

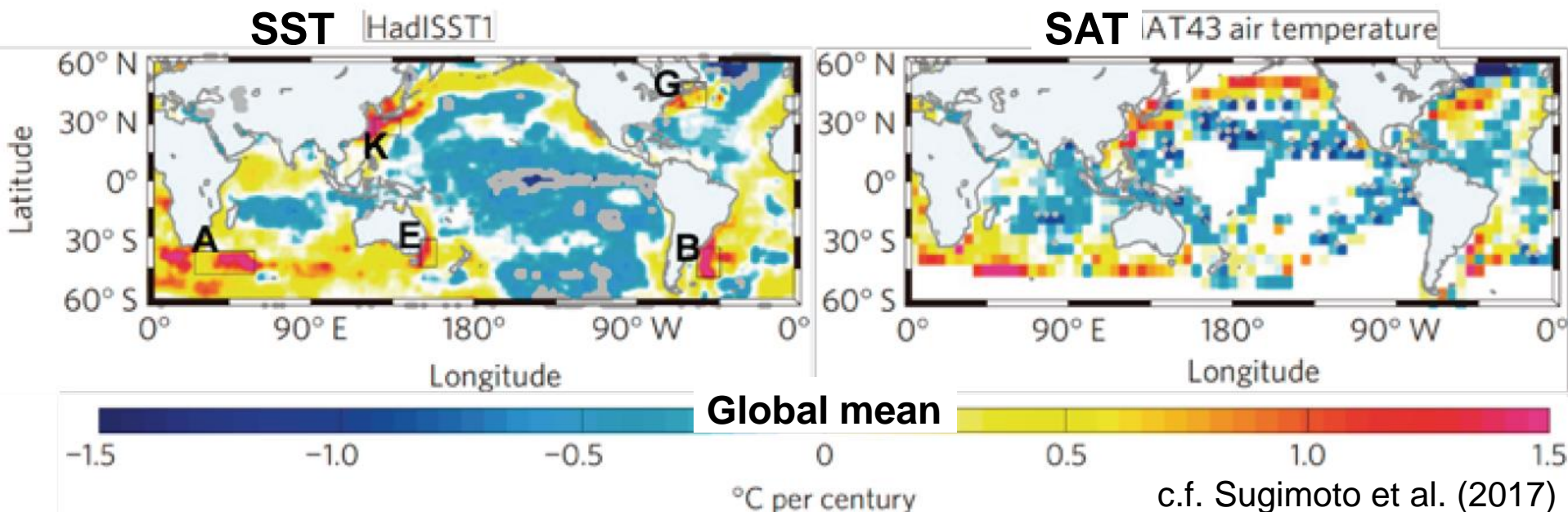


In CGCM, allowing ocean jets and eddies may enhance uncertainty, since they are generated by internal dynamics (Taguchi et al. 2007; Nonaka et al. 2015)

Enhanced warming along the western boundary currents

L. Wu, W. Cai, L. Zhang, H. Nakamura et al. (NCC 2012)

Local trend (1900~2008) as a departure from the global-mean trend



Enhanced warming around the midlatitude/subtropical warm western boundary current (WBC) regions, probably as a concentrated manifestation of wind changes through oceanic Rossby waves

Increasing importance of the WBC regions as “hotspots” in the climate system (incl. increasing risk of heavy rainfall)

Phase II of “Hotspots” in the Climate System: Another Japanese initiative on extratropical air-sea interaction study focusing on multi-scale air-sea interactions for predictability of extreme events and future climate projection

- **Phase I** (chief PI: H. Nakamura): MEXT-sponsored 5-year nation-wide project (Jul 2010~ Mar 2015) with ~65 scientists, ~10 postdocs and ~30 grad. students from meteorological and oceanographic societies.
- **Phase II** (chief PI: Masami Nonaka at JAMSTEC): Similar 5-year nation-wide project (Jul 2019~Mar 2024).



Summary and issues to be discussed (I)

1) Hemispheric/basin scales

- SST front (+moisture supply) → *stormtrack /storm intensity/ eddy-driven jet*
- Annular mode (“SST-driven” phase ↔ “internal dynamic” phase)
as variability of eddy-driven jet (PFJ)
 - ***Role of SST front in stratosphere-troposphere coupled variability***
- Decadal SST front/current variability (e.g., PDV, AMOC)
 - ocean processes (wind-driven, overturning vs. intrinsic eddy-driven)
 - **forcing basin-scale atmospheric circulation via storm track?**
(NAO, NPO or PNA) → *feedback on ocean circulation?*
- **resolution sensitivity:** atmospheric/oceanic models/ SST data
 - **Need high-resolution SST for atmospheric reanalysis**
- Roles of ocean eddies: sea-level changes, mass transports,
heat/moisture release into the atmosphere
- CMIP models/ Roles of extratropical air-sea interaction in the warmed climate

Summary and issues to be discussed (II)

2) Regional/meso-scales

- ocean front/eddies → wind convergence/divergence → clouds/convection
 - *influence onto the free troposphere?*
 - *feedback onto ocean eddies/fronts?*
- **necessity of SST data with high spatial/temporal resolution for meso-scale atmospheric simulation especially in oceanic frontal regions**
 - Atmospheric reanalysis with high-resolution SST may give us substantially different physics/energetics in how the atmosphere responds to the ocean front variability (c.f. Smirnov et al. 2015)
- influence of SST variations over the marginal seas/continental shelves on storm development/ heavy precipitation events

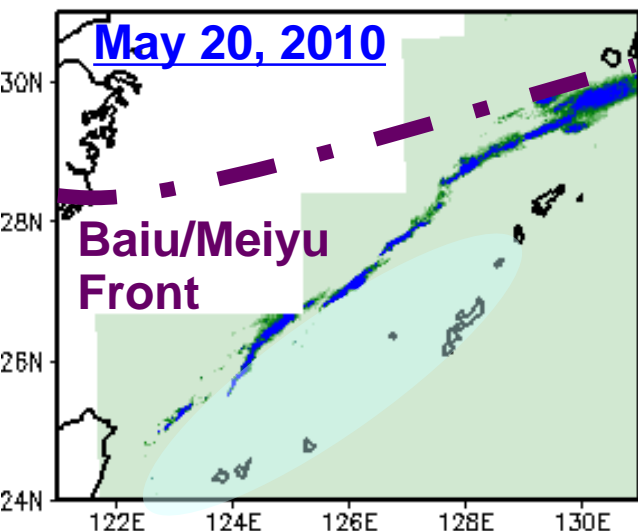
3) Micro-scales

- *Influence of warm WBCs on cloud microphysical properties via stratification?*

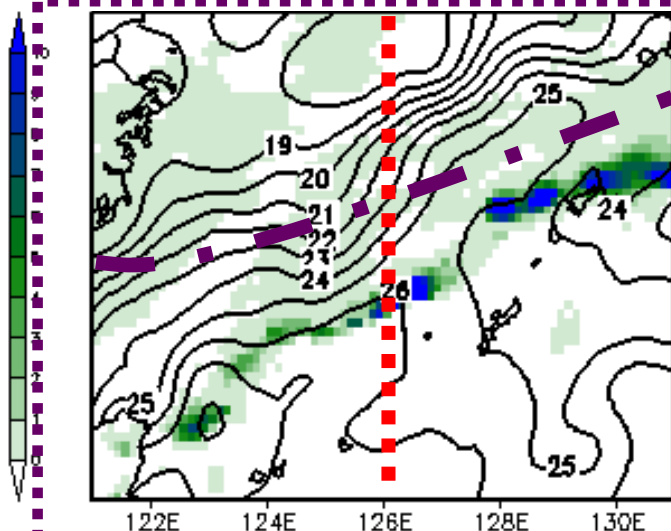
Early-summer convective rainband persistent along the Kuroshio

Miyama, Nonaka, Nakamura, Yoshida (2012, Tellus A)

radar-measured rain

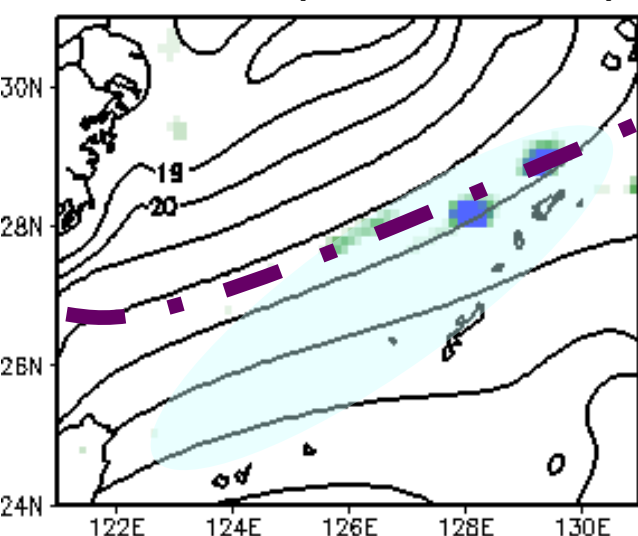


Model rain (observed SST)

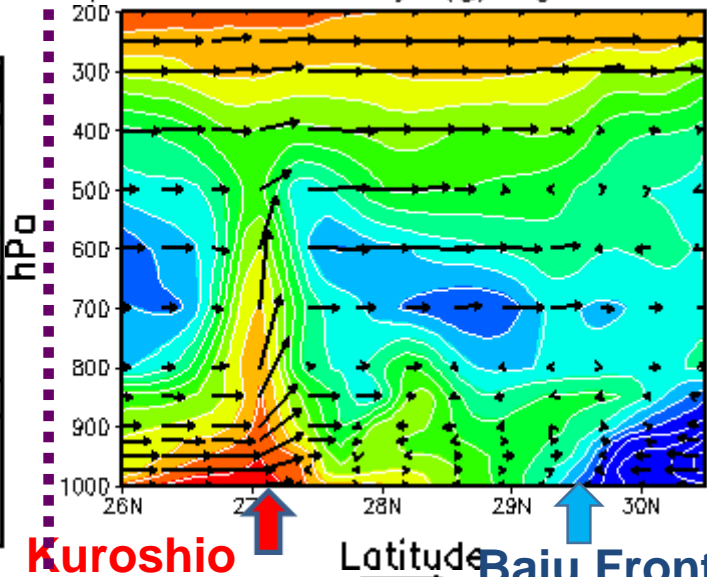


→ imprinted in June climatology of satellite precip. (Sasaki et al. 2011 JC)

Model rain (smoothed SST)



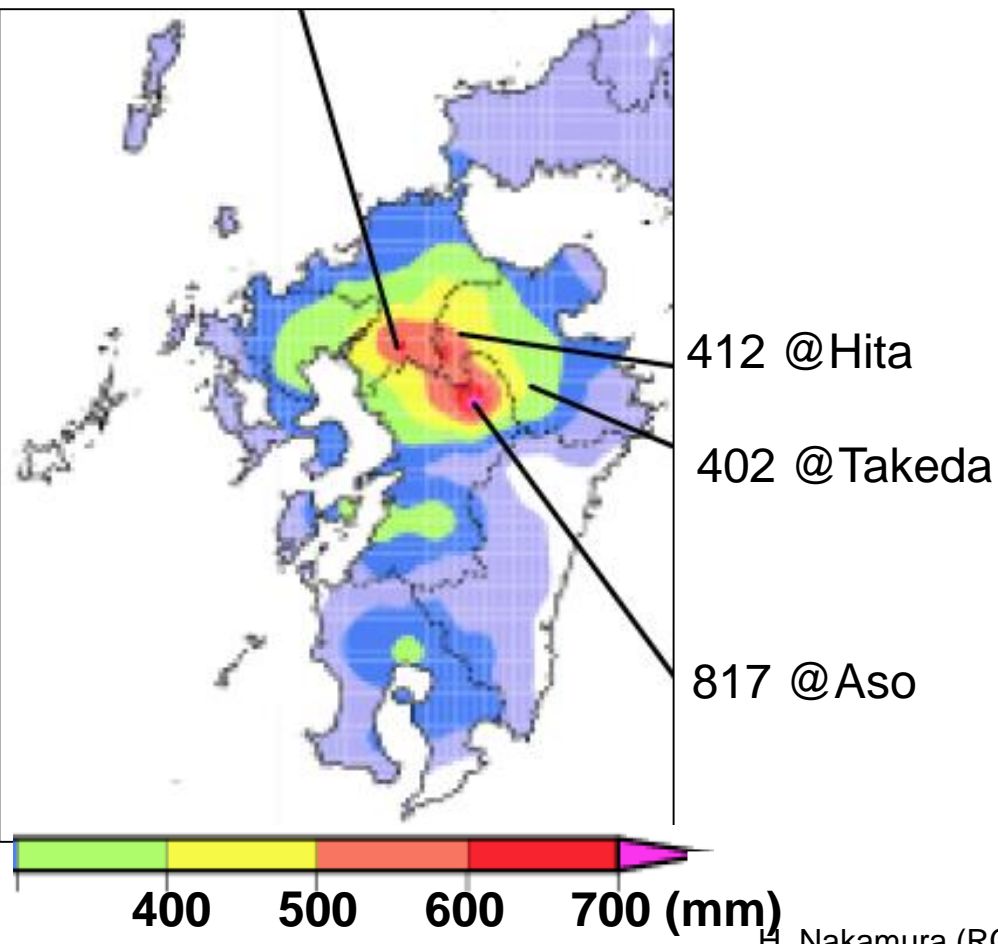
Specific humidity (g/Kg Control)



IPRC regional model fails to reproduce the primary rainband south of the Baiu/Meiyu front if SST is artificially smoothed to eliminate SST maxima along the Kuroshio

Severe flooding event over the Kyushu Island (July 11-14, 2012)

4-day total rainfall (mm) over Kyushu
649 @Kuroki



30 dead due to flooding

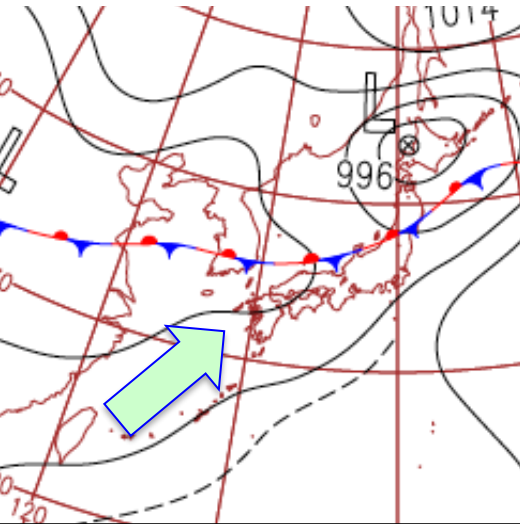


Projected increase in heavy rainfall under ocean warming

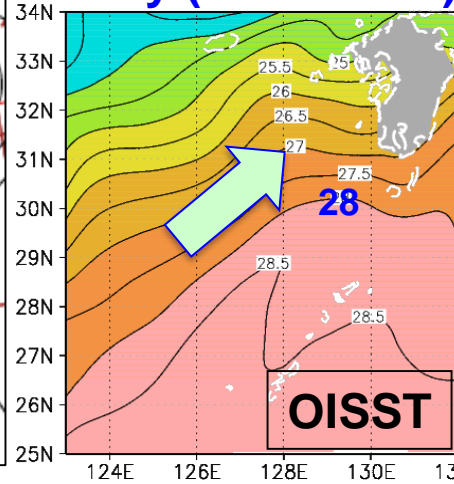
Manda, Nakamura et al. (2014 Sci. Rep.)

09JST, 13 July, 2012

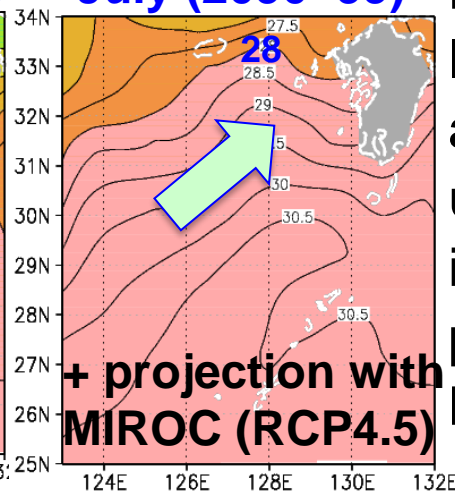
WRF (3km) experiment with the same large-scale



July (1985~2004)

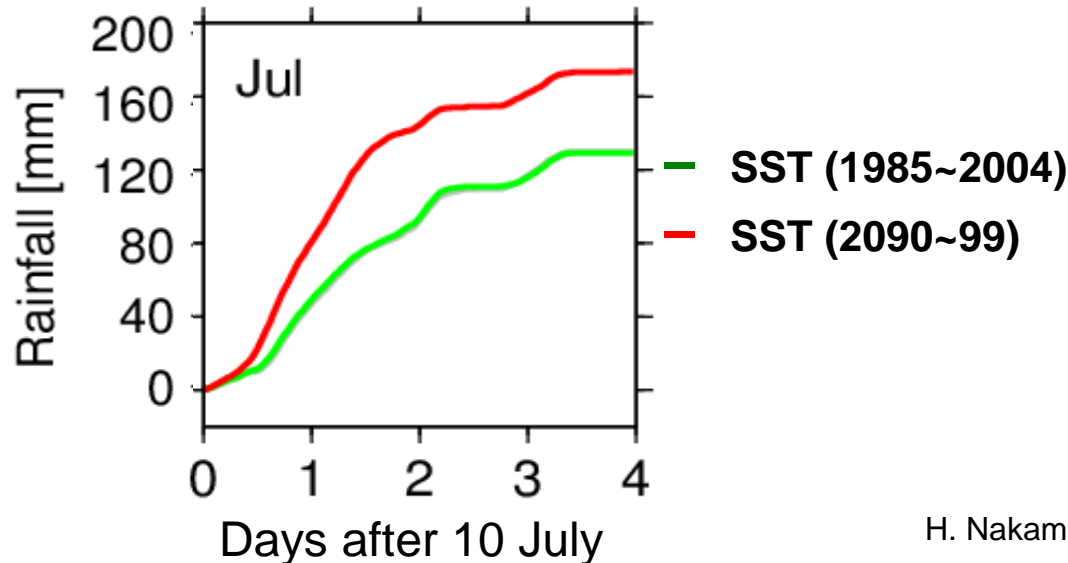


July (2090~99)



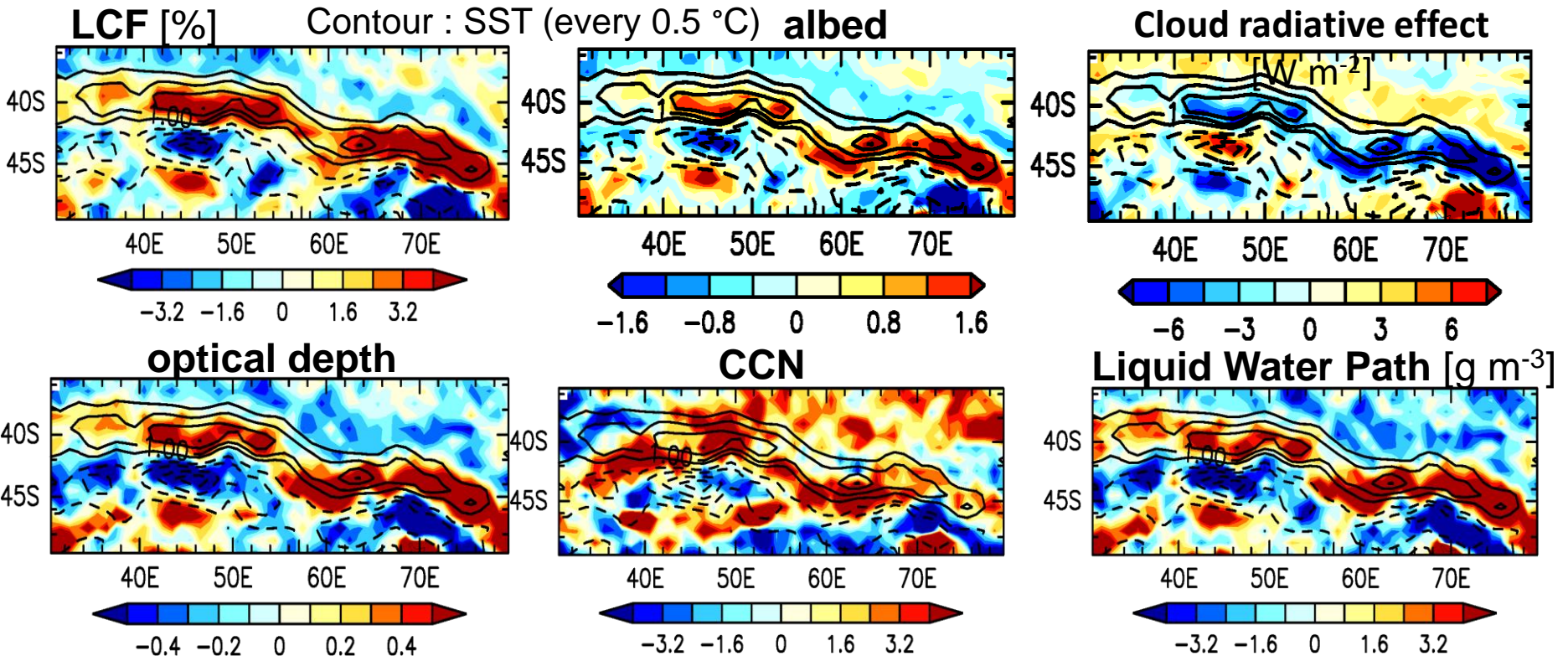
flow pattern but with local SST increment and horizontally uniform air temp. increment, both projected with MIROC5 (RCP4,5).

Accumulation of WRF rainfall averaged over Kyushu



Impact of Agulhas SST front on low-level clouds (summer)

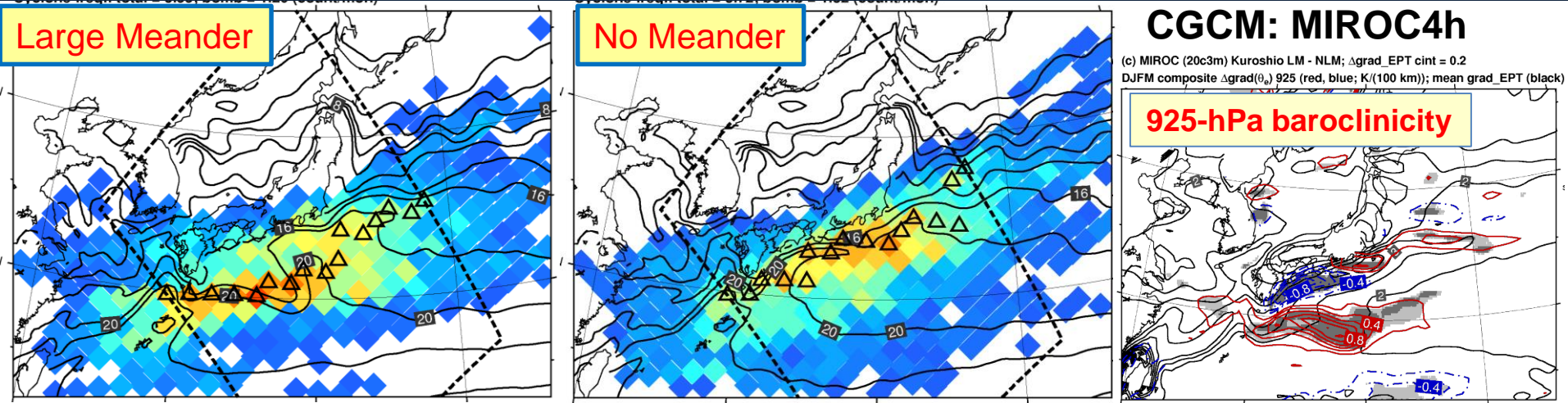
- ✓ Latitudinal $\sim 9^\circ$ high-pass filtering for highlighting impacts of the SST front



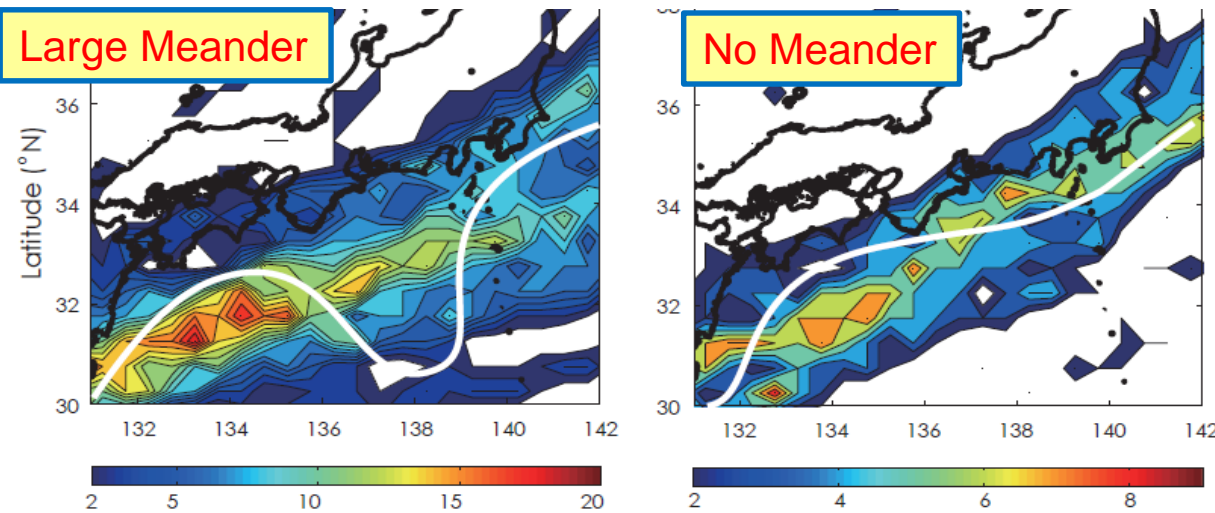
- High albedo due to enhanced optical depth arises from greater CCN and LWP, as realized especially over warm water under cold advection (Koike et al. JGR, 2012. 2016), in which ascent is enhanced for higher supersaturation level.
- Negative CRE over warmer water with higher LCF/albedo acts to weaken the Agulhas SST front.

Influence of Kuroshio Meander on wintertime cyclone tracks

R. Kawamura et al.; S. Minobe et al.



A CGCM reproduces a southward shift of the primary cyclone track during the large Kuroshio meander south of Japan, as observed (Nakamura, Minobe et al. 2012, JC).



observations

H. Nakamura (RCAST, U-Tokyo)

The large meander reduces latent heat flux south of Japan and shifts the near-surface baroclinic zone southward, thereby inhibit rapid development of cyclones in the meander region (Hayasaki et al. 2013, GRL).

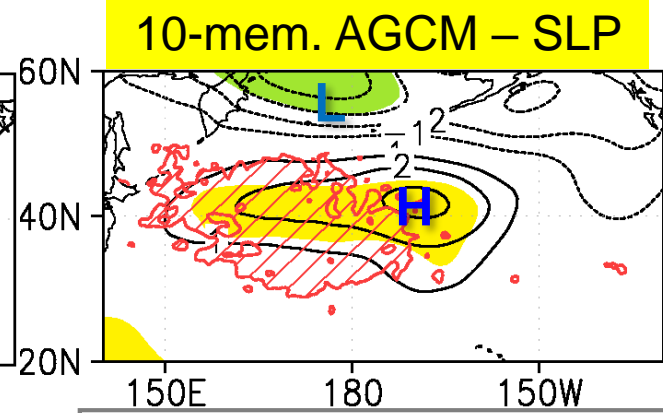
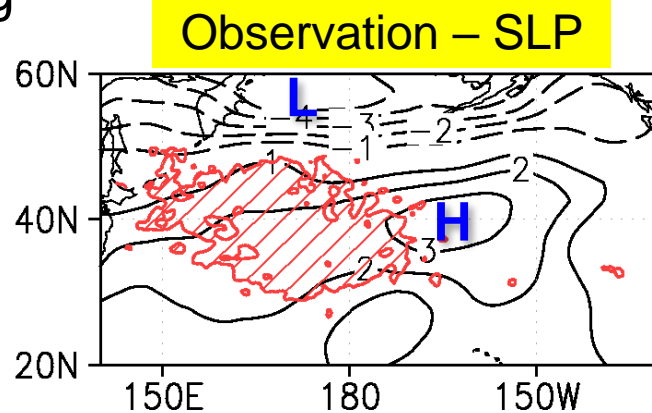
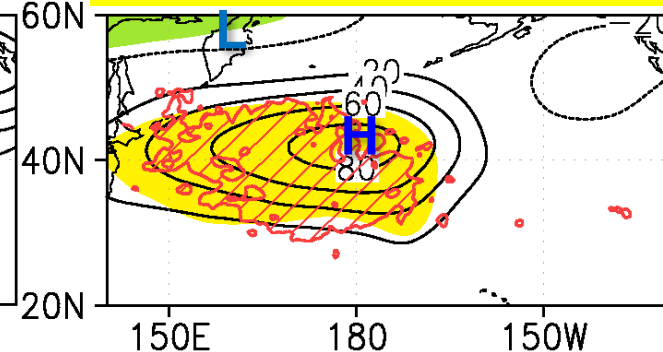
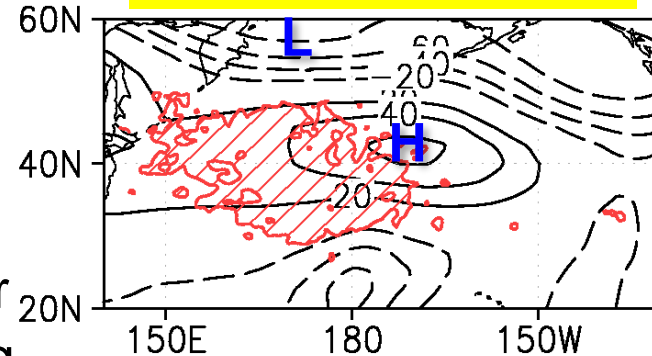
Observed and simulated circulation anomalies in October

Okajima, Nakamura et al. (2014, J. Clim.)

AGCM experiment reproduces: Observation – Z250

10-mem. AGCM – Z250

- Observed lower- and upper-tropospheric anticyclonic anomalies,
- which developed under strong feedback forcing from the poleward deflected stormtrack,



Red hatches : SSTA > +1°C

c.i. = 20m and 1hPa
Color: 95% confidence level

These atmospheric anomalies are forced by:

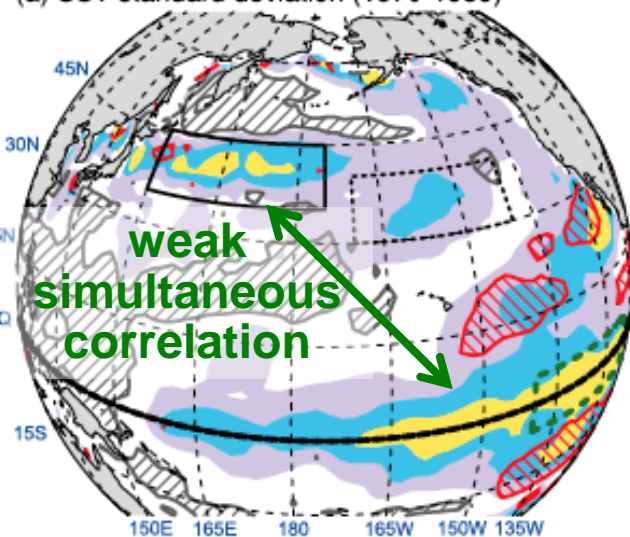
- prominent warm SST anomaly around 40°N
- associated with poleward shift and expansion of the KOE frontal zone,

Multi-decadal modulations in teleconnection from the NW Pacific

Miyasaka, Nakamura et al. (2014, GRL)

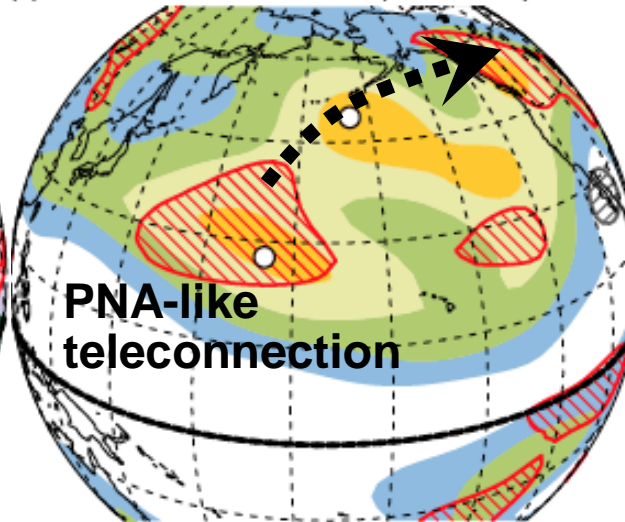
decadal SST variability

(a) SST standard deviation (1970-1989)



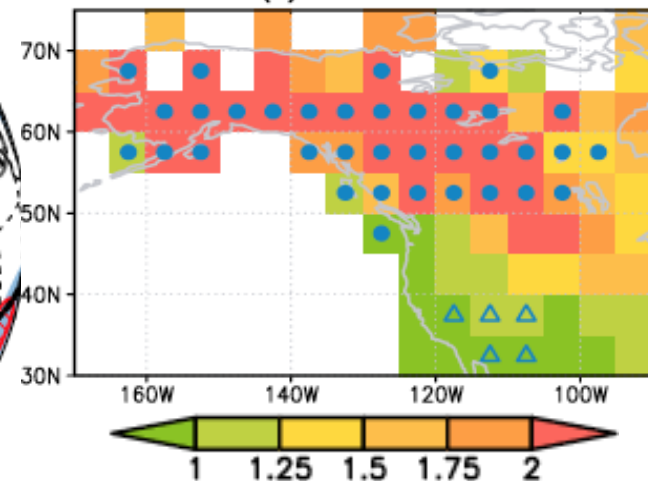
decadal 250mb height variability

(c) SF250 standard deviation (1970-1989)

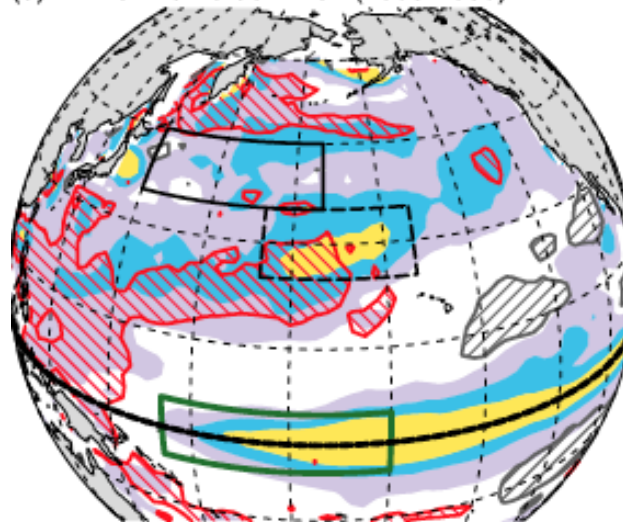


Decadal SAT variability in Alaska, Canada (DJF)

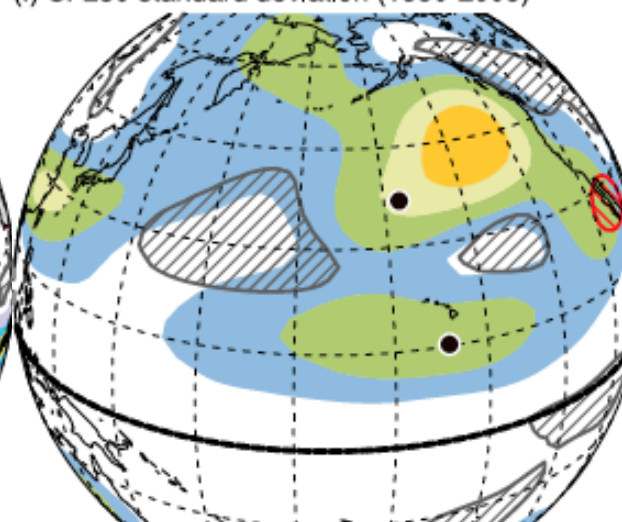
(a) 1970-1989



(d) SST standard deviation (1990-2009)



(f) SF250 standard deviation (1990-2009)



Reduced SAT variability as remote influence of weakened NW Pacific SST variability

(b) 1990-2009

